RM E53C12

NACA RM E53C12

NACA

RESEARCH MEMORANDUM

THE DESIGN OF BRITTLE-MATERIAL BLADE ROOTS BASED ON THEORY AND RUPTURE TESTS OF PLASTIC MODELS

By Andre J. Meyer, Jr., Albert Kaufman, and William C. Caywood

Lewis Flight Propulsion Laboratory
Cleveland, Ohio

NATIONAL ADVISORY COMMITTEE
FOR AERONAUTICS

WASHINGTON
April 6, 1953

NATIONAL ADVISORY COMMITTEE FOR AERONAUTICS

RESEARCH MEMORANDUM

THE DESIGN OF BRITTLE-MATERIAL BLADE ROOTS BASED ON THEORY AND RUPTURE TESTS OF PLASTIC MODELS

By Andre J. Meyer, Jr., Albert Kaufman, and William C. Caywood

SUMMARY

Theoretical design charts based on Neuber's equations for symmetrically located notches are presented for estimating the approximate rupture strengths of blade roots made from brittle materials. The limit of applicability of the theoretical charts is shown as determined by rupture tests of plastic models. The optimum proportions among over-all root width, neck width, notch radius, and notch depth are determined from the design charts.

Eighteen different root designs were investigated, their relative strengths were evaluated analytically and experimentally, and the results were compared. A dovetail root having the optimum proportions as established by this investigation was the strongest root evaluated.

INTRODUCTION

Ceramics, ceramals, and intermetallics are being investigated for turbine-blade application to conserve strategic materials and to permit operation at higher temperatures. Plastics are being considered as a compressor-blade material because they can be molded very inexpensively and because their low densities result in greatly reduced compressor weight. These new materials have very low ductility and are very sensitive to notches. As a result, the root designs used to attach blades made of conventional materials are no longer usable for fastening blades of the new brittle materials.

The purpose of the investigation reported herein is to derive a basis for designing new blade roots for brittle materials, to devise a rapid and inexpensive method of experimentally evaluating the strength of different root designs, and to propose several root designs suitable for brittle materials. Theoretical design charts showing the effects of varying the different geometric proportions of the blade root and experimental data pointing out the limitations of the theoretical

strength calculations are presented. A number of new root designs were investigated, and the results were compared with those of the standard fir-tree root now generally used in the aircraft turbine industry. The investigation was conducted at the NACA Lewis laboratory.

SYMBOLS

The following symbols are used in this report (for clarification of some of these symbols refer to fig. 1.):

D	over-all width of blade root below notch = 2h + d
d	minimum width or neck distance between notches
h	notch depth
K_f	general stress-concentration factor for arbitrary notch depth
k_d	stress-concentration factor for deep notch
k_s	stress-concentration factor for shallow notch
P_r	rupture load of specimen
r	radius of notch, groove, or fillet
S_t	tensile strength of blade material at operating temperature
t	thickness of model

THEORETICAL BASIS FOR BLADE-ROOT DESIGN

The blades of a compressor or a turbine are primarily loaded in tension because of the strong centrifugal forces acting on the blade mass at the high rotational speeds normally encountered in a jet engine. Actually the blades are also loaded in bending because of the gas forces, but the gas forces are of relatively low magnitude when compared with the centrifugal forces. Furthermore, the bending stresses caused by the gases can be neutralized through careful design by offsetting the center of gravity of the airfoil with respect to the center of the cross-sectional area at the root neck. The bending loads therefore were neglected throughout this blade-root investigation.

Blades are generally attached to the high-speed rotors by engaging projections on the rotor with grooves or notches in the blade root. This arrangement results in both tensile and compressive stresses occurring

in close proximity in the notch of the blade root. Although extensive investigations have been completed to determine the effect of notches in tension, bending, and torsion, the literature does not include the type of loading found in the blade root. The closest approximation is provided by the case of pure tension, as covered by many investigators (refs. 1 to 9). Neuber has derived the following equations to determine the stress-concentration factors for symmetrical hyperbolic-shaped notches subjected to tension (ref. 1, p. 170):

$$k_s = 1 + 2\sqrt{\frac{h}{r}} \tag{1}$$

$$k_d = \frac{2\left(\frac{d}{2r} + 1\right)\sqrt{\frac{d}{2r}}}{\left(\frac{d}{2r} + 1\right) \arctan\sqrt{\frac{d}{2r}} + \sqrt{\frac{d}{2r}}} \tag{2}$$

$$K_f = 1 + \frac{(k_s - 1)(k_d - 1)}{\sqrt{(k_s - 1)^2 + (k_d - 1)^2}} \tag{3}$$

These equations have been confirmed experimentally by Frocht (refs. 2 and 3) and others for specimens with notches of constant radius rather than the hyperbolic notch. The stress-concentration factors derived by Neuber are valid only in the elastic range; however, for ideally brittle materials, the elastic range extends to the point of fracture and therefore the theory should be applicable to the immediate problem.

The primary consideration in designing any blade root is the magnitude of the load that the root will carry without failure. The rupture load is given by

$$P_r = \frac{dtS_t}{K_f}$$

For a given rotor, t is relatively constant and is mainly determined by the chord at the base of the airfoil. The tensile strength S_t also is constant for a given blade material, and therefore d/K_f is directly proportional to the rupture load of the blade root. In many of the graphs presented, the ordinate will be d/K_f divided by D to obtain the parameter d/DK_f, which will be called the load factor throughout the remainder of this report. The load factor d/DK_f then must simply be multiplied by the over-all width D, the thickness t, and the tensile strength S_t to obtain the theoretical rupture load.

By assigning arbitrary values to the dimensionless parameters h/D and r/D, Neuber's equations can be used to establish a single basic family of curves. Dividing h/D by r/D gives values for h/r which, when substituted in equation (1), enables k_s to be determined. From the geometry of symmetric specimens it is obvious that the over-all width D is given by the neck distance plus twice the notch depth or

$$D = d + 2h$$

Dividing by D gives

$$1 = \frac{d}{D} + \frac{2h}{D}$$

$$\therefore \frac{d}{D} = 1 - \frac{2h}{D}$$

Thus, from the arbitrary values already selected for h/D, d/D is readily determined. Dividing d/D by $2r/D$ results in $d/2r$, the only parameter needed in equation (2) to obtain k_d. Then, K_f can be determined by equation (3), which, when divided into d/D, gives the load factor d/DK_f. This procedure was followed to construct the basic curves in figure 2. These curves are not the most convenient form for all design purposes, however, because the effect on the load factor of varying certain parameters and holding other parameters constant is not readily apparent. Figures 3 and 4, which show the theoretical effect of varying the proportions of a blade root, can be easily derived by cross plotting from the basic curves of figure 2.

For pin-type roots (semicircular notches) the ratio of notch radius to notch depth r/h is constant once the magnitude of the included angle between the sides of the root has been established. Figure 3(a), constructed by using straight lines radiating from the apex of figure 2 as illustrated by the 45° line $r/h = 2$, therefore shows how the load factor is affected by r/D for several constant values of r/h. The curve $(r/h = 1)$ shows the relative load-carrying capacity of parallel-sided roots with semicircular notches (notch depth equals notch radius) of various radii. For each curve of constant r/h ratio, there is an optimum value of r/D; for example, it can be seen that the theoretical optimum value for r/D is 0.15 for the parallel-sided semicircular notches. For a given D value, smaller radii result in high stress-concentration factors, thus reducing the load capacity. Larger radii reduce the neck distance d and thereby reduce the load capacity by decreasing the cross-sectional area carrying the load. For the shallower notches the optimum r/D value is not longer 0.15, but increases as the notch depth decreases.

In figure 4(a) is a graph of the same information presented in figure 3(a) except that the load factor is plotted against h/D as the

abscissa instead of r/D. As indicated by the nearly vertical locus passing through the peaks of the various r/h curves, the optimum value of h/D for given values of r/h is relatively constant, varying from only 0.09 to 0.15 over the wide range of notch depths considered. Because the neck distance d is equal to $D - 2h$, the optimum value of d/D lies between 0.7 and 0.82 regardless of the notch radius.

By cross plotting with the horizontal straight lines of figure 2, figure 3(b) is derived and it shows the important effect on the load factor of varying r/D for constant values of h/D. For given values of over-all width D and notch depth h, the load factor increases continually as the notch radius r increases, at first very rapidly when r is small and then more gradually.

For completeness, the effect on the load factor of varying r/D for constant values of r/d is shown in figure 3(c). The effect of varying the notch depth h for constant values of r and D is shown in figure 4(b). This figure is derived by cross plotting the vertical straight lines of figure 2. Obviously, the shallower the notch depth, the greater will be the load capacity of the root. Theoretically, the limiting load factor in this direction is 1.0 because the theory is based on simple tension. When loading occurs in the notch, however, further limitations are imposed because sufficient bearing area must be provided to avoid excessive compressive stresses, and substantial shoulders must be incorporated to prevent the blade from pulling out of the rotor by plastic flow of the rotor material. The importance of bearing area was investigated experimentally and will be discussed in the section Practical Limit of Design Charts.

Based on these theoretical design charts, the following general conclusions can be summarized:

(1) The neck distance should be between 70 and 82 percent of the over-all root width, which consequently limits the notch depth h to between 9 and 15 percent of the over-all width for a fixed value of r/h.

(2) The notch radius should be as large as possible as long as the neck distance is not sacrificed to obtain increased notch radius.

(3) The notch depth should be as shallow as practical when r/h can be freely varied, providing sufficient bearing area is maintained.

Interpolation in figures 3 and 4 is difficult. For greater convenience, charts were constructed to a larger scale (superposition of figure 3 drawn four times size), and copies may be obtained through a written request to the NACA. The load factor may easily be interpolated from the alinement chart presented in figure 5. This chart covers only the more important area of the graphic design charts and does not show

the trends caused by changing the variables as do the graphic illustrations, but it is easier to use. The load factor can be estimated to the third decimal place by drawing a straight line through the known r/D and h/D or d/D ratios. Another alinement chart is needed to determine directly the load factor for known values of r/d or r/h, but the ratios used in figure 5 can be readily calculated from r/d or r/h ratios.

Two additional approximate design charts showing the effect of changing either the notch radius or the neck distance independently of D and h are included in appendix A. These two charts enable the designer to approximate the load factor when only r and d are known in any convenient units of length.

ROOT STRENGTHS EVALUATED BY TENSILE TESTS

Experimental Technique

The design charts presented in the preceding section of this report are based on the theory for notched bars in pure tension. While blade roots are loaded primarily in tension, the loading is applied in the notch; thus, part of the notch surface is subjected to very high bearing stresses while other parts of the notch surface slightly removed from the contact area are highly stressed in tension. In order to find what effects this loading arrangement has on rupture strengths and to find the limits of applicability of the design charts, it was necessary to conduct rupture tests on a large number of specimens in order to cover the important ranges included in the charts. A transparent methyl methacrylate plastic was chosen as the specimen material because it is readily available in a convenient form, it is easily machined with simple tools, and it possesses the brittle qualities that were being investigated. This plastic also has the added advantage in that it has photoelastic properties which are useful in indicating unsymmetrical loading. Also, high photoelastic fringe concentrations denote points of high stress concentration to be alleviated by design changes.

More than 400 specimens were fabricated and tested to obtain the data presented herein. About half this quantity were basic notched specimens which did not simulate blade roots, while the other half were used to compare the strengths of various blade-root profiles. In all cases presented, the results of at least three specimens were averaged to establish a data point.

The first group of models were parallel-sided, semicircular notched specimens of varying notch radius. One series was pulled in tension. For comparison, a second series was tested in which the loading was applied at the notches, as would be the case for blade roots. In another

group of models, notch radius was maintained constant and width was progressively reduced in order to show the limitations of bearing loads. Many more specimens of this type but with a wide range of notch radius and notch depth were tested; and, although the results were not plotted independently, they were compiled with the actual root specimens showing the same trends.

Several additional root specimens were fabricated to determine the effects of other variables such as the included angle between sides of the profiles and the effects of additional lands used to distribute the load.

Specimen Fabrication

Eighteen different root designs were devised and proportioned in accordance with the theoretical design charts. The profiles of these roots, some of which have been in common use for a long time, are sketched in figure 6 and the pertinent dimensions of each model are listed in table I. In order to obtain a fair comparison of root design strengths, all roots were proportioned on the basis of inserting 54 blades in a rotor with a diameter of 18 inches and a thickness of 1.96 inches. The mass of the airfoil (4.25 in. long) and its platform were assumed to be equal for each root design, and the rotor segments between blades were designed to have approximately equal strength in all cases. In order to facilitate handling and machining, the root models were all made 2.2 times the exact size.

The specimens were cut on a jig saw to within 0.05 inch of the final profile and then were routed to final shape on a high-speed router (10,000 rpm) with various diameter cutters. The routing was accomplished by two techniques. When small fillets and radii (less than 0.080 in.) were needed, an accurately machined steel template was followed by the blind end of the routing cutter, as photographed in figure 7(a). Larger fillets and radii were produced by pivoting the model about a stationary center which engaged a plastic template drilled with only the accurately located centers of the desired radii, as illustrated in figure 7(b). A blast of air was directed at the cutter during routing to prevent overheating of the specimen material.

Loading Apparatus

The plastic specimens are provided with wedge-shaped bearing surfaces which engage self-centering tapers of the loading fixtures. Several pinned linkages are incorporated in the loading fixtures to facilitate symmetrical loading about the center line of the specimen (fig. 8(a)). To prevent spreading of the specimen component representing

the rotor segment, an adjustable clamp made of photoelastically insensitive plastic was fastened around the mating specimen pieces. In some cases, a fixture in which various-diameter aluminum cylinders could be installed was used to grip the notched specimens so that a new specimen piece corresponding to the rotor segment did not have to be made for each test (fig. 8(b)). A 10,000-pound universal hydraulic testing machine was used for loading specimens, while the conventional polariscope surrounded the specimen, thus allowing the projected fringe patterns to be observed during loading (fig. 9). Unsymmetrical loading was corrected by slight adjustment of the loading fixture.

RESULTS AND DISCUSSION

In order to ascertain the applicability of the simplified theory in evaluating and predicting strength of the different root configurations, the plastic models were pulled to destruction. The plastic sheet material, nominally 1/2 inch thick, was used as received, however, although the thickness varied from 0.465 to 0.570 inch. The rupture loads reported for both the simple notch specimens and the blade root specimens were adjusted for variations in thickness.

Notch Specimens

The design charts presented earlier in the report (figs. 3 and 4) are based on a theory for notched bars in pure tension; and, while blade roots are loaded primarily in tension, the loading is applied in the notch, a condition not covered by theory. In order to justify the application of the simplified theory to blade roots, a number of specimens with a constant over-all width of 1.5 inches, and with one series loaded in the notch and the other series loaded as specified by theory, were ruptured and compared. The results are shown in figure 10. The simple tensile specimens show a higher strength than would be predicted by Neuber's theory, but a parallel trend is indicated. Apparently, the plastic material is not completely lacking in ductility, although the ordinary means of measuring ductility would show zero ductility.

The curve for the specimens with load applied at the notches correlates closely with the theoretical curve for values of r greater than 0.4 inch. For values of r less than 0.4 inch, the experimental curve illustrates the importance of providing sufficient bearing area. As the notch radius and consequently the notch depth decreases, the model can no longer carry the high load predicted by theory. If the experimental rupture load is divided by the notch depth, an approximately linear relation occurs as plotted. The notch depth is directly proportional to the bearing area since the thickness is constant.

In order to prove that reduced bearing area is the cause of loss in load capacity rather than failure of the theory to predict the load capacity of various notch radii, a second group of specimens of constant notch radius was tested. Variations in bearing area were accomplished by reducing the width of the model below the notch. Again the rupture load as shown in figure 11 dropped rapidly as the notch depth decreased below 0.2 inch. Above a notch depth of 0.2 inch the rupture load is higher than predicted by theory, but the experimental results are parallel to the theoretical curve for this case. When the rupture load is divided by the notch depth, a curve similar to that in figure 10 is obtained. These curves in figures 10 and 11 are used in the section Practical Limit of Design Charts to determine the useful limits of the theoretical design charts.

Blade-Root Specimens

For convenience in design, the charts of figures 3 and 4 include all five parameters r/d, d/D, r/D, h/D, and r/h. Any two can be used to determine the load factor d/DK_f, which then merely must be multiplied by the over-all width D, the thickness t, and the tensile strength S_t to obtain the theoretical rupture load. The load factor and the theoretical rupture load for each design investigated are included in table I. The experimental rupture load (an average of at least three specimens), and the percent deviation are also listed. It can be seen that the notch theory is capable of predicting the rupture load only within about ± 20 percent, but this accuracy is not too poor when the great differences in design configurations are considered. The number of load-carrying lands, for example, vary from 2 to 12, and about half the designs incorporated interposing pieces between the blade and rotor components. The largest part of the discrepancies probably arise, however, from the lack of perfect homogeneity of the specimen material. With brittle materials, minute defects, nicks, and scratches have pronounced effects on rupture strengths. Seemingly perfect specimens of identical models vary considerably (± 10 percent) in their rupture loads.

Blade-Root Design Procedure

The design procedure is illustrated in figure 12, which is a duplicate of the design charts (fig. 3) superimposed on one sheet, including the design points of the various root designs.

Fir-tree designs. - The three- and the six-serration designs are typical of proportions used for metal turbine blades and are included for comparative evaluations. As would be expected because of the very small notch radii, the design charts show a low load factor. The actual rupture load is relatively high because the over-all width D at the top

serration is inherently the highest obtainable with any design. The modified fir-tree, two-serration root was specifically designed for brittle materials in accordance with the design charts. The high D was retained and the notch radii were greatly increased, thus attaining one of the highest theoretical rupture loads of all the designs (table I). The specimens, however, consistently failed at the lower neck at a reduced rupture load. The lower blade-root neck could not be widened without reducing the width of the wheel segment between blades and thus overstressing the turbine rotor.

Pin designs. - The pin designs were proposed primarily because a relatively soft and ductile material could be inserted between the blade and rotor material to prevent uneven load distribution over the surface of the brittle blade material. Secondly, these designs are more easily fabricated in production.

On the basis of stress distribution in both the rotor and the blade root, the included angle of the pin in shear-type roots (semicircular notches) was selected to be 37°, thus fixing the ratio r/h equal to 1.46. The pin root design proportions were determined by remaining close to the peak of the $r/h = 1.46$ design curve. The two-pin design resulted in low theoretical rupture loads because the pin removes cross-sectional areas normally available for carrying tensile loads in the blade root or in the rotor or both. The four-pin design provides a larger D while the load factor is also slightly increased (fig. 12) and this design still permits sufficiently strong rotor segments. The six-pin design provides a still larger rupture load by increasing D even though the load factor drops slightly, as shown on figure 12.

The two-pin root with pins in compression again illustrates the importance of providing sufficient bearing area. The neck distance and pin diameter are the same as the two-pin-in-shear-type root, but the experimental rupture load is 10 percent higher as a result of adding more bearing area. It is interesting to note that the experimental rupture load of the pin-in-compression model is about equal to the theoretical rupture load of the two-pin-in-shear design. The same improvement can probably be made in the four- and six-pin models, but it is questionable if the slight improvement would warrant the added machining complication. For the pin-in-compression-type root it is difficult to ascertain the effective D because the thin edges cannot support any load.

The staggered-pin design is the final pin-type root investigated. By alternately staggering the pins, it was hoped to increase the rupture load by reducing the cross section removed by pins at a given radius of the rotor. This design, however, inherently has a lower load factor (fig. 12), and the experimental rupture load is still lower probably because of the introduction of bending loads resulting in very nonuniform load distribution at the neck of the root. Actually the design charts

do not apply for this case because the charts are based on symmetrically located notches. However, the accuracy is as good as in other cases. The theory for notches on only one side of a plate would predict a lower rupture load agreeing more closely with the experimental load for the staggered-pin root.

Dovetail designs. - Dovetail model A was proportioned so as to be close to the peaks of the r/h curves on the design chart (fig. 12) and to provide what appeared to be reasonable bearing shoulders and notch depths. Dovetail B was an exploratory design in which the theoretical load factor of design A was retained, while the notch radius and notch depth were increased by reducing the neck distance. The experimental rupture load averaged 12 percent higher for model B than for model A and is higher than for any other root discussed thus far. This increase is not predicted by theory and the reason for the increase is not understood.

Interlock designs. - The interlock design is a very promising configuration because it permits very large notch radii in the root without introducing small radii, and consequently high stress concentrations, in the rotor segments. It utilizes a soft ductile material between rotor and blade, and is self-centering according to the loads acting upon the blade because it can rotate slightly in its socket. The interlock design should be the easiest of all the roots to fabricate both for blades and for the rotor recesses. The radii of the blade-root notch and the rotor socket were made equal in the models investigated, although they may, of course, be of different values if advantageous for particular cases. The proportions chosen for interlock A gave the highest theoretical load factor attained and one which correlated well with experimental results.

Interlock B was designed to obtain an increased over-all width D. The bearing area was increased while the neck distance d was kept constant. It was realized, however, that the load factor would be reduced (fig. 12). The experimental rupture loads agreed very well with the theoretical predicted value, but were much lower than for interlock A.

Interlock C was an attempt to increase the rupture strengths of interlock A by adding load-carrying lands. The first specimens consistently ruptured between the two pins. In the second group of specimens the pin diameter was reduced slightly to reduce the load carried by the pins, but still the rupture loads were lower than for interlock A, even though an occasional failure occurred simultaneously at the upper neck. The lower failure load is probably explained by the instantaneous shock loading applied to the upper neck, which causes the upper neck to rupture immediately after the lower neck breaks.

Ball and wedge roots. - As noted in appendix B, an appreciable increase in rupture load is theoretically possible if a fillet rather than a notch is used. The ball and wedge roots lend themselves to fillets and therefore were investigated. They cannot be proportioned to obtain high load factors on the design charts. The ball-root design is poor because this design is very prone to pull out of the rotor, particularly with larger radii at the neck. The wedge root with large radius reduces essentially to the form of the dovetail and no longer retains its flat-loading-surface characteristic of the wedge design.

These designs were reproportioned with the intention of staggering adjacent roots (long, short, long, short, etc.) as was done in early turbosuperchargers, thus allowing all root dimensions to be increased. This procedure did produce an increased rupture load, but also the operating loads were higher because of the extended neck and subsequently increased blade mass. This principle was also analytically investigated for the dovetail and interlock designs, but the net theoretical gain was negligible and did not warrant the added complication.

Practical Limit of Design Charts

A definite relation was noted between the notch depth and rupture load divided by the bearing area for the simplified notch specimens (figs. 10 and 11). Plotting the data points for different specimens on a single graph (fig. 13) showed that all the points fell closely together in a single envelope. There is no correlation between notch radius, neck distance, or any other factor and the position of the data point (high or low) in the envelope. Since the specimens tested include a thorough coverage of all the design variables, it is doubtful that additional specimens could be made to appreciably exceed the upper boundary of the envelope of figure 13. This upper-boundary curve then becomes the limit beyond which the bearing stresses exceed the capabilities of the material. These data, of course, apply directly only for the methyl methacrylate plastic, but the limit curves for other materials should be very similar. It is doubtful that the limit curve of any other truly brittle material will have much higher values than for the plastic chosen, because the ductility of the plastic, though slight, is greater than the ductility of the other brittle materials. The rupture load is given by

$$P_r = \frac{dtS_t}{K_f}$$

The parameter used in figure 13 is P_r/Dht, which therefore equals dS_t/hDK_f. Thus, in order to obtain the load factor used in the design charts (figs. 2, 3, 4, and 12),

$$\frac{d}{DK_f} = \left(\frac{P_r}{Dht}\right)\left(\frac{h}{S_t}\right)$$

The factor P_r/Dht must be multiplied by the corresponding notch depth h and divided by the tensile strength S_t of the material. This has been done with the limit curve in figure 13 to obtain the limit curve in figure 14 by dividing by S_t = 12,000 pounds per square inch, which is very close to the average S_t experimentally determined for over 20 unnotched tensile bars.

The maximum theoretical load factor that can thus be expected is 0.462. In other words, the maximum rupture load (in pounds) attainable per inch of root thickness and per inch of over-all width for the plastic models is 46 percent of the tensile strength of the specimen material expressed in pounds per square inch. The dimensional ratios established by the optimum point are

$$r/D = 0.45,\ h/D = 0.175,\ r/h = 2.54,\ d/D = 0.650,\ \text{and}\ r/d = 0.69$$

Because of the horizontal flatness of the limit curve in this region, these ratios can be varied appreciably without a reduction in load factor. Figure 14(a) shows that for h/D greater than 0.175, increases in the notch radius for given h and D values result in continual increases in the rupture load (following the constant h/D curves) until intersection with the limit curve, after which there is a gradual decrease in load capacity following the limit curve. Figure 14(b) indicates a rapid increase in the rupture load for any given notch radius and over-all width (r/D constant) as the notch depth decreases up to the point where the bearing stresses become excessive (intersection of r/D curve and limit curve) and thereafter a rapid drop in rupture load for further decreases in the notch depth.

The theoretical load factor of interlock A is slightly greater than the theoretical maximum attainable value on the basis of bearing load, and it is interesting to note that the load factor computed from experimental rupture loads is 0.454, or slightly below the theoretically maximum attainable load factor. The only root configuration other than the interlock type which lends itself to these optimum ratios is the dovetail design. A dovetail root therefore was proportioned to match the optimum ratios. This root is shown in figure 6 as dovetail C. The exact dimensions used are included in table I. Tensile tests of this optimum root resulted in the highest rupture load reached by any of the blade models, thus substantiating the usefulness of the design charts and the limit curves.

Effect of Included Angle on Dovetail Root

The effect of varying the included angle between sides of the dovetail root below the notch was checked for detrimental effects. The included angle was varied on a series of specimens from 0° (parallel sided) to 120° while all other dimensions were held constant. As illustrated by the data points in figure 15, within the range investigated, the effect of included angle, if any, was far overshadowed by the scatter of the experimental rupture loads.

Effect of Additional Load-Carrying Lands

A series of six-serration fir-tree specimens was fabricated; and perfect matching between blade and root components was produced by observing the photoelastic fringe patterns under light loads, removing the high spots, and repeating this process until all teeth appeared to be approximately equally stressed. Then varying numbers of teeth were removed. The results of tensile tests on these specimens are plotted in figure 16. First, from the figure it can be seen that the rupture load is a linear function of the number of teeth remaining. Secondly, it will be noticed by observing the two types of data points in the figure that the matched 12-tooth roots ruptured at higher loads (averaged 3526 pounds) than the models made with normal precautions, thus corresponding to standard production-line machining tolerances (averaged 2439 pounds). The matched 12-tooth models fractured at even higher loads than predicted by theory (2570 pounds) according to table I and higher than would be indicated by the bearing-stress limit curve (for the same r/D, fig. 14, the limit curve gives a load factor of 0.282, which corresponds to a rupture load of 3020 pounds). This increase as well as the linear relation is due to the decreased bearing stresses, bearing stresses being inversely proportional to the number of teeth actually carrying the load. The limit curve is based on a single pair of load-carrying lands and multiland roots of normal tolerance where the loads are probably also carried by a single pair of lands. Therefore, it would appear beneficial to incorporate additional load-carrying lands provided mating parts are extremely accurately machined or are hand-fitted. It should be emphasized, however, that the rotor and blade components were made from the same plastic material, and the tests were conducted at room temperature. If the rotor were made from a conventional turbine material and the blades were made of a brittle ceramic, ceramal, or intermetallic compound, then even if the matchings were perfect upon assembly, considerable mismatching would result under operating loads and temperatures because the moduli of elasticity, the rotor and blade stresses, and the component temperatures all would be different. If these effects could all be accounted for in the design stage for a particular operating speed and condition (such could be done only for one speed and power condition), then it may not be possible to assemble

the precision parts in the cold static state. One possible means of overcoming some of these difficulties in the use of brittle blade materials is to insert a soft ductile shim material between the blade root and the rotor. The soft material should then deform under load, taking up whatever dimensional difference may exist or develop.

The fact that the four-pin and six-pin roots carry more load than the two-pin root cannot be attributed to the additional lands. The theoretical strength is based on only the dimensions of the neck closest to the airfoil. This neck alone could take the experimental loads attained. Additional lands are necessary in these cases, however, because if all the load is transmitted through the top land alone, the wheel segment between adjacent blades would fail at very low loads.

CONCLUDING REMARKS

Based on the theoretical analysis and on the rupture tests of plastic specimens, it was found that the theory for simple notches loaded in tension was applicable for estimating the strength of blade-root models loaded in the notches except when the bearing stress became excessive. The design charts constructed according to the notch theory for symmetrically notched plates loaded in tension are capable of predicting the actual rupture loads of the plastic blade-root models within about ±20 percent regardless of the size or depth of the notches or the number of lands carrying the load.

The optimum root proportions were established as determined by the limiting compressive stresses the material can withstand, and the blade root designed to have these proportions showed the greatest strength of the 18 different designs tested. The investigation furthermore revealed that the net strength of roots cannot be increased appreciably by staggering adjacent roots at different radial distances from the rotor axis. Although the load capacity of the roots is increased by staggering, the operating loads acting on the roots are also increased, resulting in a negligible net gain.

The use of more than a single pair of load-carrying lands to increase the rupture strength of root designs does not seem to be practical with brittle materials because of the extreme machining accuracy required.

SUMMARY OF RESULTS

The following results were derived from a theoretical and experimental investigation conducted to facilitate the design of roots for blades to be made from brittle materials:

1. For pin-type roots where the ratio of notch radius to notch depth is a constant, the maximum theoretical rupture load is obtained when the neck distance is between 70 and 82 percent of the over-all width and consequently the notch depth is between 9 and 15 percent of the over-all root width.

2. Decreasing the notch depth for a given over-all root width and notch radius will continually increase the rupture load up to the point where the bearing stresses become excessive, after which the rupture load drops very rapidly.

3. Increasing the notch radius for a given notch depth and over-all root width increases the load capacity of the root until excessive bearing stresses cause a gradual decrease in load capacity.

4. A limit curve, based on the compressive stress at rupture of the plastic models and independent of notch size or depth, was established which indicated the range of usefulness of the design charts.

5. The optimum root proportions as established by the limit curve are: The notch radius should be 69 percent of the neck distance; the notch radius should be 45 percent of the over-all root width; and the notch radius should be 2.54 times the notch depth.

6. A dovetail-type root proportioned in accordance with the optimum ratios attained the highest strength.

7. The interlock-type root required the next highest load to produce failure, second only to the dovetail roots.

Lewis Flight Propulsion Laboratory
National Advisory Committee for Aeronautics
Cleveland, Ohio

APPENDIX A

SIMPLIFIED DESIGN CHARTS

The design charts presented in the body of the report (figs. 3 and 4) are exact plots of Neuber's equations. The assumption that for all roots the notch depth h equals the notch radius r or $r/h = 1$ introduces only a small error in rupture load even for very deep or very shallow notches unless the notch radius is very small. If the relation $h = r$ is used, the family of curves for constant values of the ratio D/d as ordinarily presented (refs. 3 and 5 to 9) reduces to the single curve for semicircular notches shown by the upper solid line curve in figure 17. The error that is introduced by assuming $h = r$ for deep notches up to $h = 10r$ and for shallow notches with a depth equal to one half the notch radius is shown by the spread in K_f outlined by the two dashed curves. An error of less than 10 percent is introduced for all values of r/d greater than 0.2, which is well within the scatter band of experimental data. Values of r/d less than 0.2 would never result in a good design for brittle materials.

By cross plotting from the curve for $h = r$ (fig. 17), the simplified design curves of figure 18 are obtained. Figure 18(a) shows directly the effect on load capacity of varying only the notch radius for constant values of neck distance d. From these curves it can be seen that, when r is small, large increases in rupture load will result from increasing r; however, when r is large, appreciable changes in r will not greatly affect the final rupture load.

In figure 18(b), the other important variable, neck distance d, is plotted against the load factor d/K_f for constant values of notch radius. The load-carrying capacity of the root increases steadily as the neck distance increases; and as the neck distance becomes large, this relation becomes linear and of approximately equal slope for the different values of r. Obviously d should be made large, but its magnitude is limited by the size of the rotor and the number of blades that must be installed in the rotor.

The number of blades to be used per rotor is largely designated by the aerodynamic considerations. For a given rotor, then, the value of D is relatively constant and roughly equal to the rotor circumference at radial location of blade-root necks divided by twice the number of blades required. Since D is thus established, both r and d cannot be permitted to vary independently of D. Furthermore, though these charts permit the designer to estimate the rupture load without deciding on the notch depth, the limiting-load capacity based on compressive stresses is directly a function of notch depth and therefore cannot be noted on these figures. For these reasons the most useful design charts, though not so simple to use, are those presented in the body of the report (figs. 3 and 4).

APPENDIX B

INCREASED LOAD CAPACITY BY USE OF FILLETS

Another possible means of increasing the load-carrying capacity of blade roots, particularly roots with relatively small notch radii, is indicated by the experimentally established curve for fillets (fig. 17). The curves for both fillets and notches are shown for comparison, and an appreciable improvement is noted over the notched root of the same radius if a fillet is used between the range of r/d from 0.05 to 0.45. These results suggest providing a straight section at the base of the notch, which condition approximates that for fillets. Generally, however, the advantage of the fillet is offset by the added weight and consequently increased centrifugal force produced by the lengthened blade-root neck.

REFERENCES

1. Neuber, H.: Theory of Notch Stresses: Principles for Exact Stress Calculation. Trans. No. 74, David Taylor Model Basin, Navy Dept. Nov. 1945.

2. Frocht, Max M.: Factors of Stress Concentration Photoelastically Determined. Jour. Appl. Mech., vol. 2, no. 2, June 1935, p. A-67.

3. Frocht, Max M.: Photoelastic Studies in Stress Concentration. Fillets, Holes, and Grooves in Tension, Compression, and Bending. Mech. Eng., vol. 58, no. 8, Aug. 1936, p. 485.

4. Seely, Fred B., and Dolan, Thomas J.: Stress Concentration at Fillets, Holes, and Keyways as Found by the Plaster-Model Method. Bull. No. 276, Eng. Exp. Sta., Univ. of Ill., June 1935.

5. Lemaire, D. A.: A Review of Some Basic Types of Geometric Stress Concentration. Report ACA-48, Aero. Res. Consultative Comm., Australia, Sept. 1949.

6. Frocht, M. M.: A Photoelastic Investigation of Stress Concentrations Due to Small Fillets and Grooves in Tension. NACA TN 2442, 1951.

7. Frocht, M. M.: Factors of Stress Concentration in Bars with Deep Sharp Grooves and Fillets in Tension. Proc. Soc. Exp. Stress Anal., vol. VIII, no. 2, 1951, pp. 149-162.

8. Peterson, R. E.: Design Factors for Stress Concentrations. Part 2 - Notches and Grooves in Tension and Torsion. Machine Design, vol. 23, no. 3, Mar. 1951, pp. 161-165.

9. Durelli, A. V., and Jacobson, R. H.: Factors for Stress Concentration in Bars with Deep Sharp Grooves and Fillets in Tension. Proc. Soc. Exp. Stress Anal., vol VIII, no. 2, 1951, pp. 163-170.

TABLE I. - BLADE ROOT PROPORTIONS AND LOADS

[For profiles see fig. 6.]

Design	Notch radius, r, in.	Neck distance, d, in.	Over-all width, D, in.	Notch depth, h, in.	r/d	r/D	d/D	h/D	r/h	Theoretical load factor, d/DK_f	Theoretical rupture load, P_r, lb	Experimental rupture load, P_r, lb	Percent deviation
3-Serration fir tree	0.074	1.493	1.931	0.195	0.050	0.038	0.773	0.113	0.338	0.234	2711	2385	-12.0
6-Serration fir tree	.055	1.500	1.785	.143	.037	.031	.840	.080	.385	.240	2570	2439	-5.1
Modified fir tree	.296	1.208	1.767	.280	.245	.168	.684	.158	1.06	.356	3774	3257	-13.7
2 Pin in shear	0.225	0.630	0.938	0.154	0.357	0.240	0.672	0.164	1.46	0.402	2262	1917	-15.3
4 Pin in shear	.243	.897	1.231	.167	.271	.197	.729	.136	1.46	.404	2984	2693	-9.8
6 Pin in shear	.175	1.170	1.410	.120	.150	.124	.830	.085	1.46	.398	3367	3013	-10.5
2 Pin in compression	.225	.630	1.406	.438	.357	.160	.448	.312	.514	.232	1957	2225	13.7
Staggered pins	.242	.770	1.012	.242	.314	.239	.761	.239	1.00	.330	2004	1605	-19.9
Dovetail A	0.345	0.961	1.452	0.246	0.359	0.238	0.662	0.169	1.40	0.397	3459	3715	7.4
Dovetail B	.563	.800	1.443	.322	.704	.390	.554	.223	1.75	.396	3429	4204	22.6
Dovetail C	.652	.943	1.449	.253	.631	.450	.651	.175	2.58	.462	4017	4681	16.5
Interlock A	0.687	0.834	1.307	0.237	0.824	0.526	0.638	0.181	2.90	0.474	3715	3555	-4.3
Interlock B	.413	.834	1.434	.300	.495	.288	.582	.209	1.38	.379	3261	3256	-.2
Interlock C	.687	.834	1.307	.237	.824	.526	.638	.181	2.90	.474	3715	2935	-21.0
Ball root A	0.134	0.666	1.331	0.333	0.201	0.101	0.500	0.250	0.402	0.240	1917	2307	20.4
Ball root B	.250	.813	1.625	.406	.308	.154	.500	.250	.615	.279	2720	3047	12.0
Wedge root A	.132	.792	1.188	.198	.167	.111	.667	.167	.667	.306	2180	2540	16.5
Wedge root B	.132	1.137	1.533	.198	.116	.086	.742	.129	.667	.306	2815	2743	-2.55

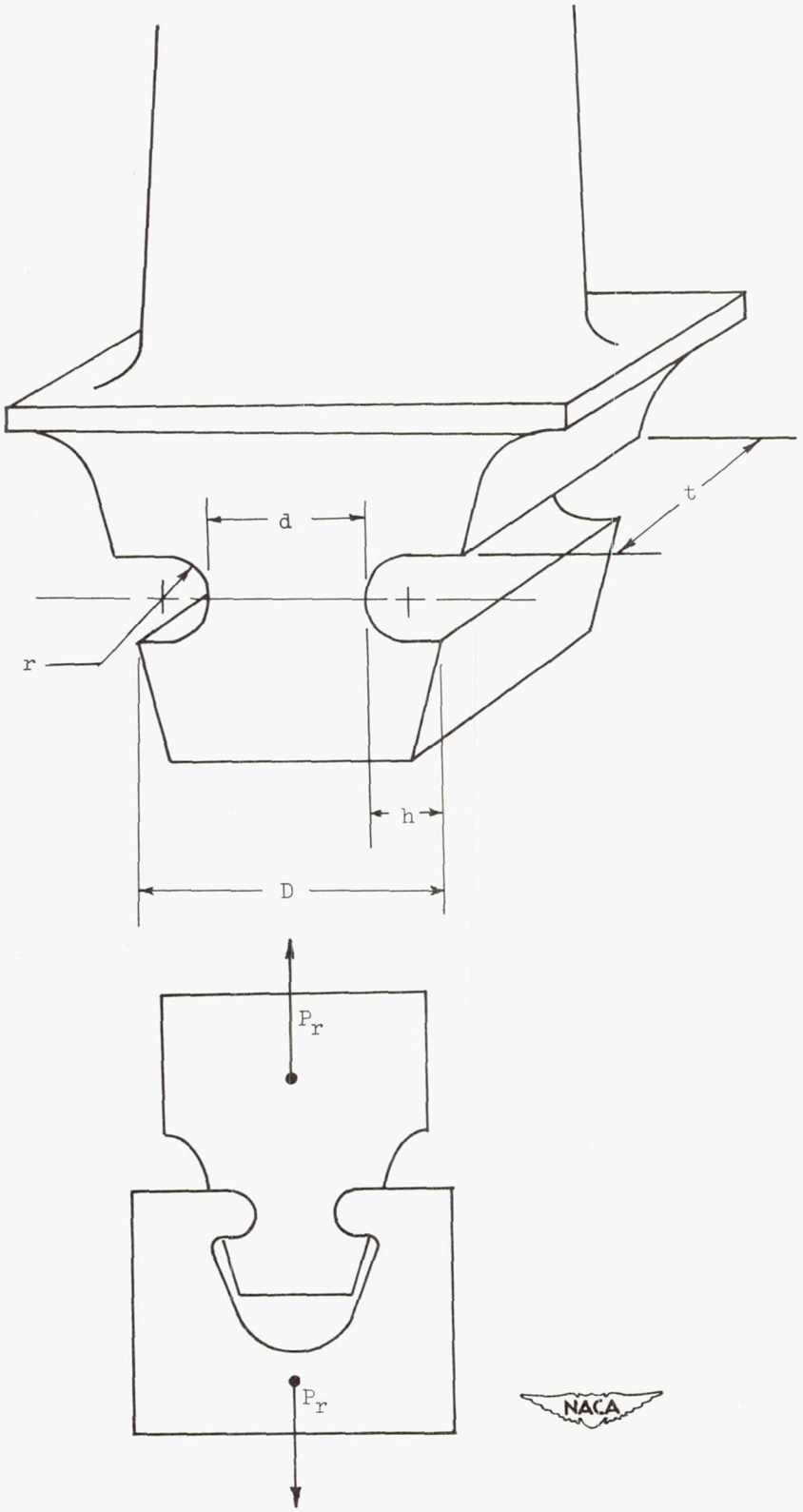

Figure 1. - Definition of symbols.

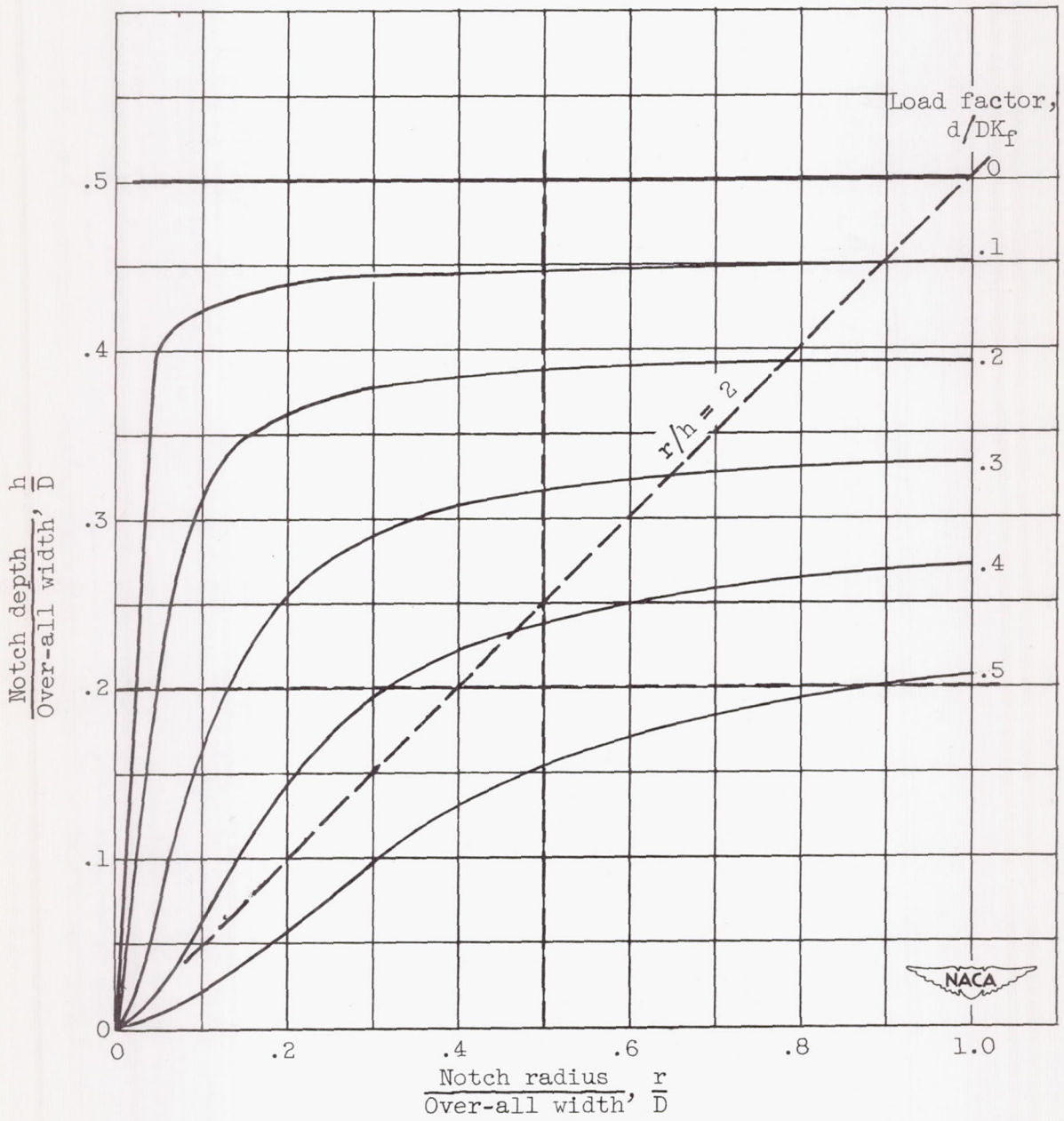

Figure 2. - Basic curves determined from Neuber's equations.

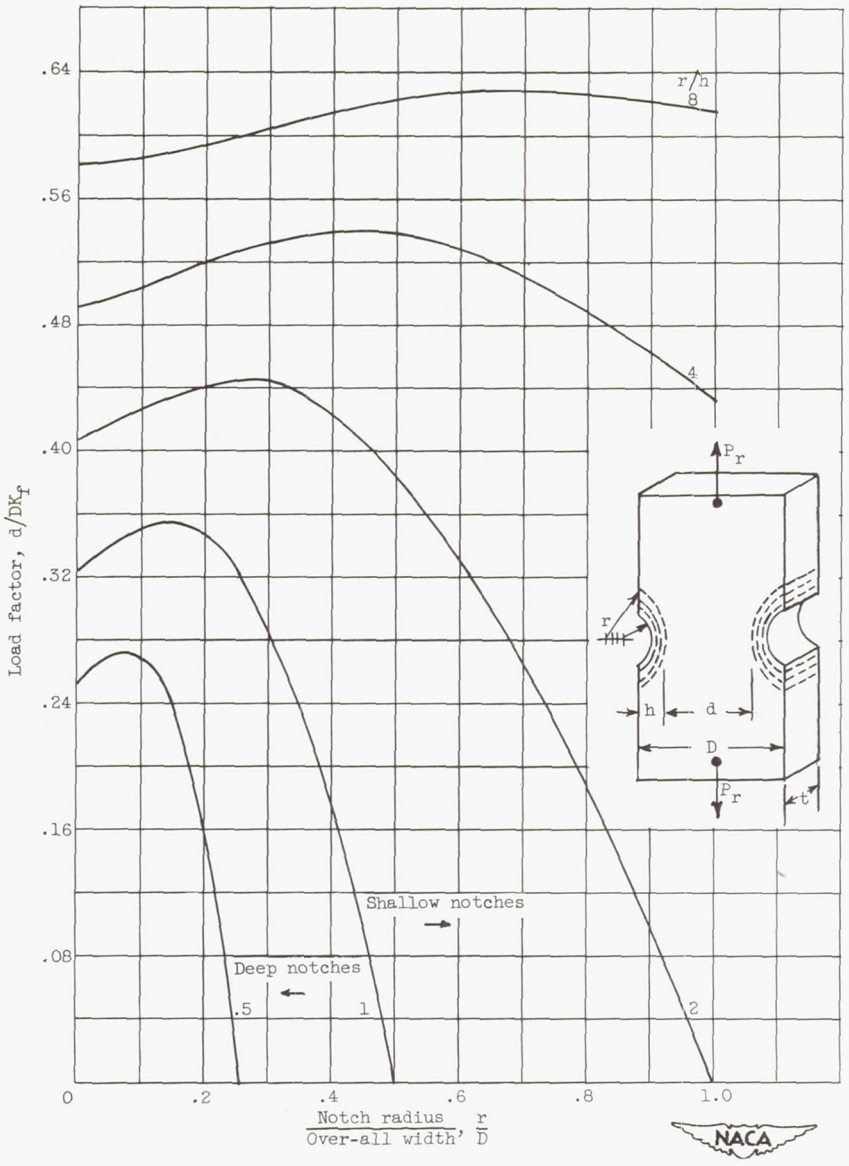

(a) Parameter r/h constant.

Figure 3. - Theoretical charts for design of brittle-material blade roots based on Neuber's equations (load factor against notch-radius parameter). $P_r = \frac{d}{DK_f} tDS_t$. S_t, tensile strength.

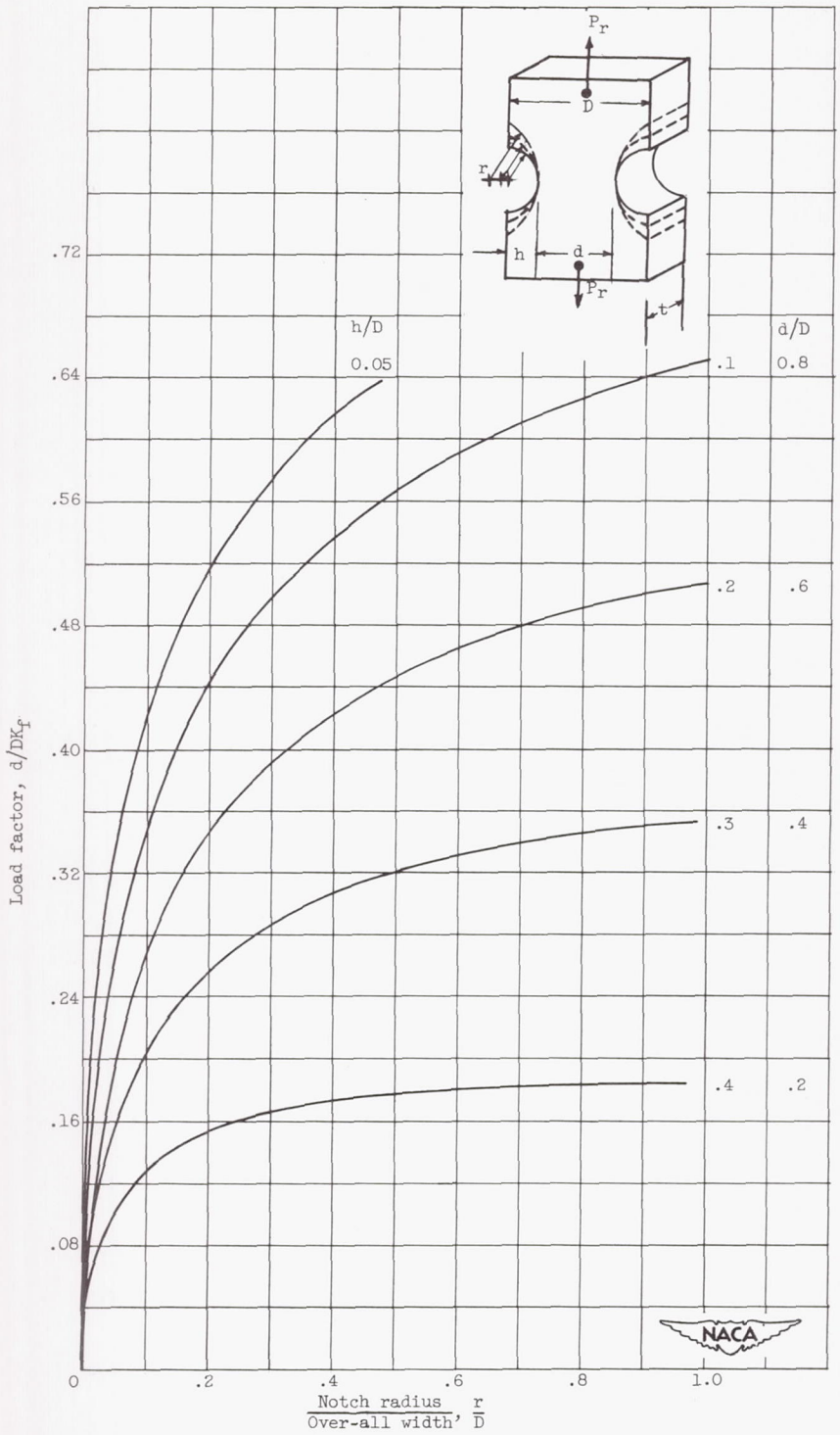

(b) Parameters h/D and d/D constant.

Figure 3. - Continued. Theoretical charts for design of brittle-material blade roots based on Neuber's equations (load factor against notch-radius parameter). $P_r = \frac{d}{DK_f} tDS_t$. S_t, tensile strength.

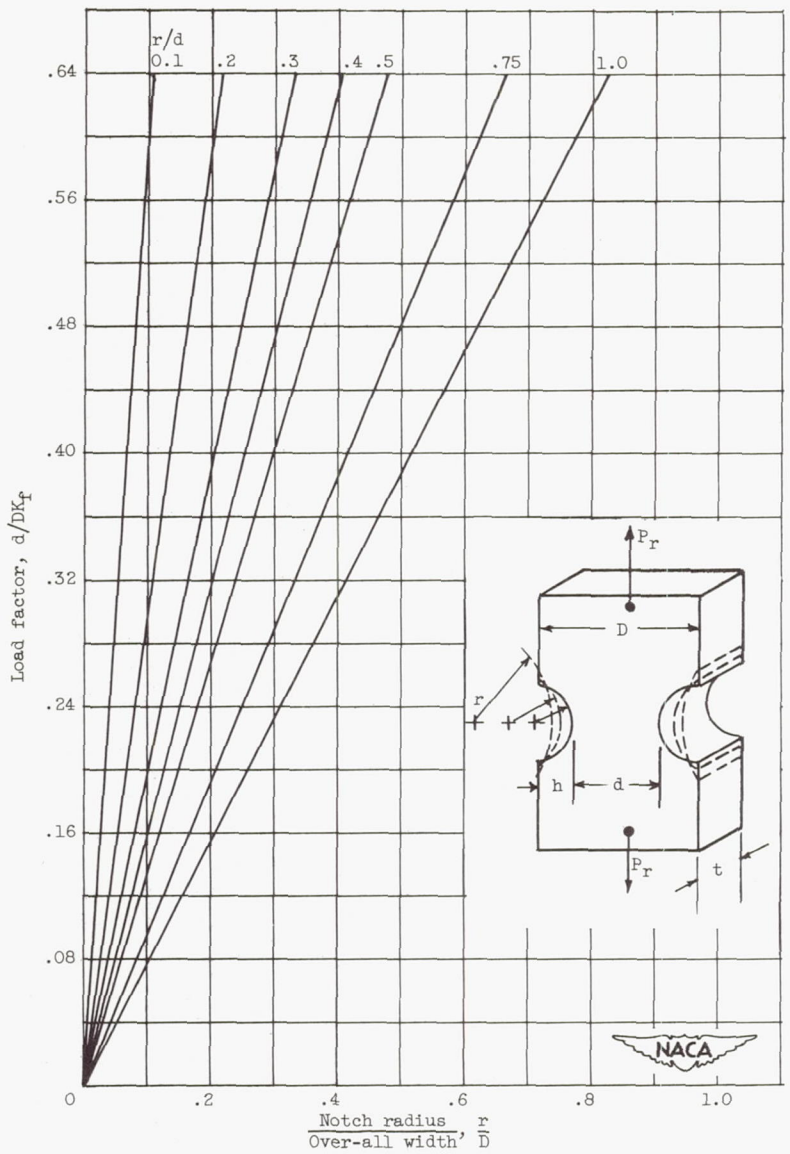

(c) Parameter r/d constant.

Figure 3. - Concluded. Theoretical charts for design of brittle-material blade roots based on Neuber's equations (load factor against notch-radius parameter). $P_r = \frac{d}{DK_f} tDS_t$. S_t, tensile strength.

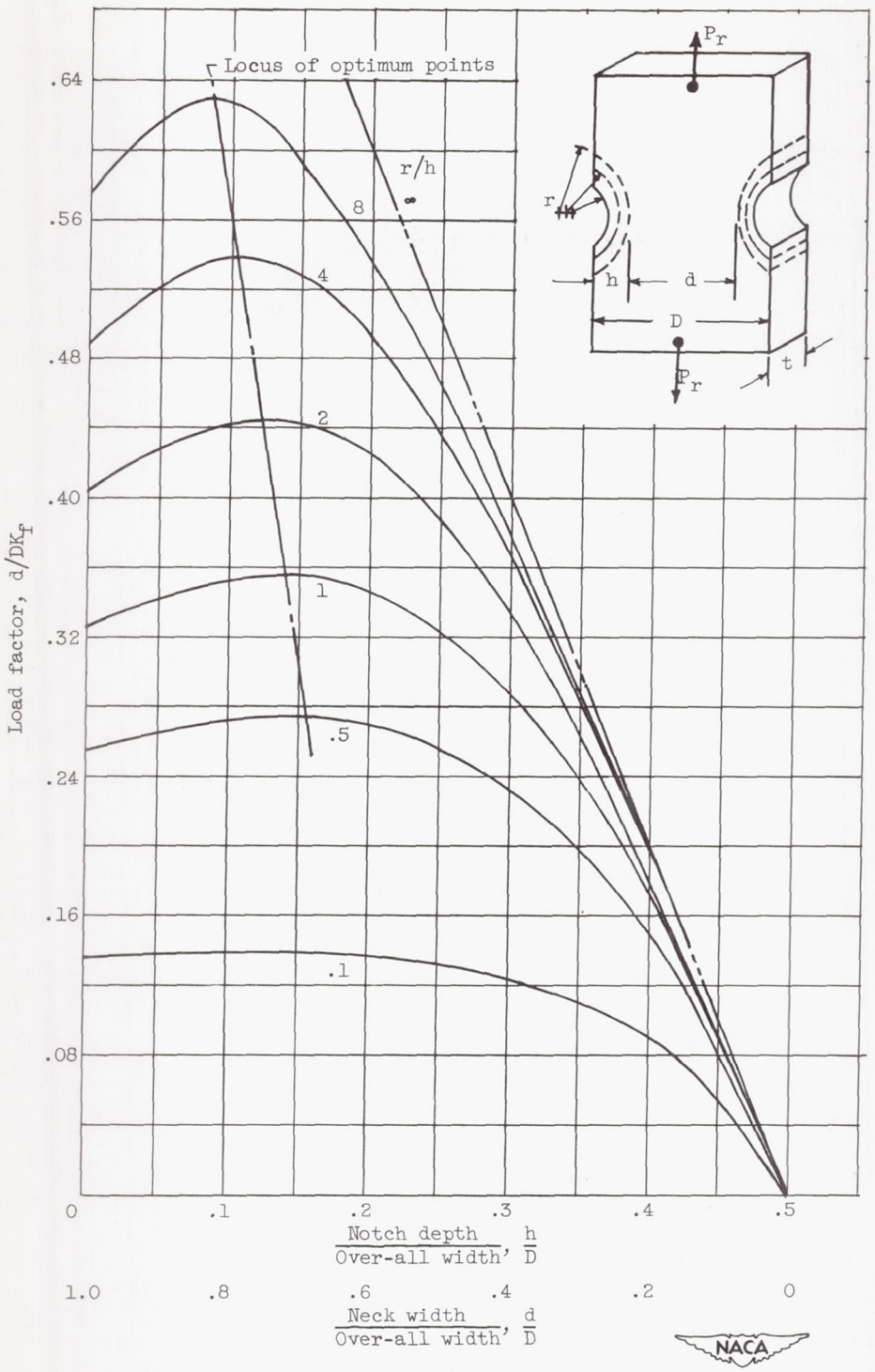

(a) Parameter r/h constant.

Figure 4. - Theoretical charts for design of brittle-material blade roots based on Neuber's equations (load factor against notch-depth parameter). $P_r = \frac{d}{DK_f} tDS_t$. S_t, tensile strength.

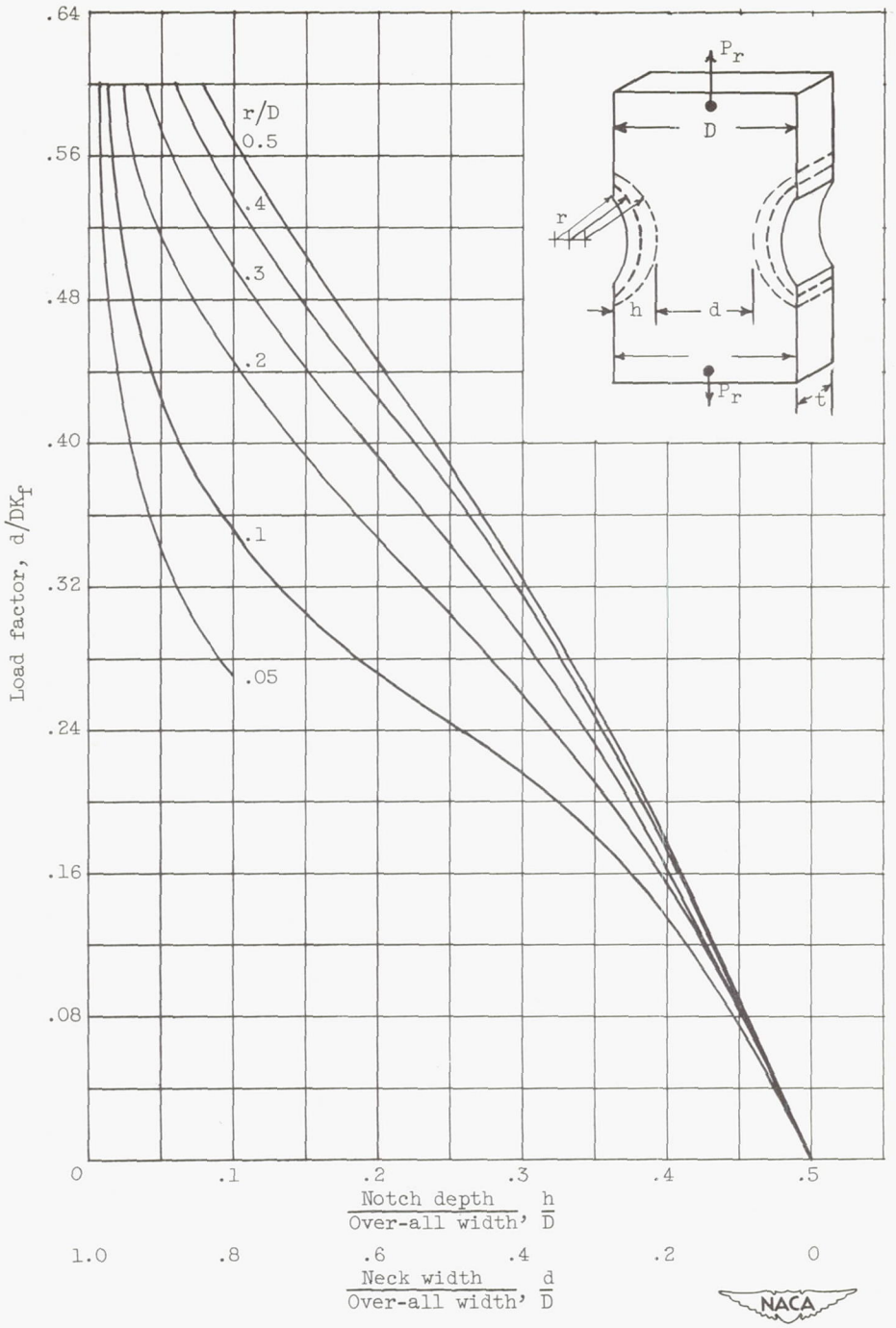

(b) Parameter r/D constant.

Figure 4. - Concluded. Theoretical charts for design of brittle-material blade roots based on Neuber's equations (load factor against notch-depth parameter). $P_r = \frac{d}{DK_f} tDS_t$. S_t, tensile strength.

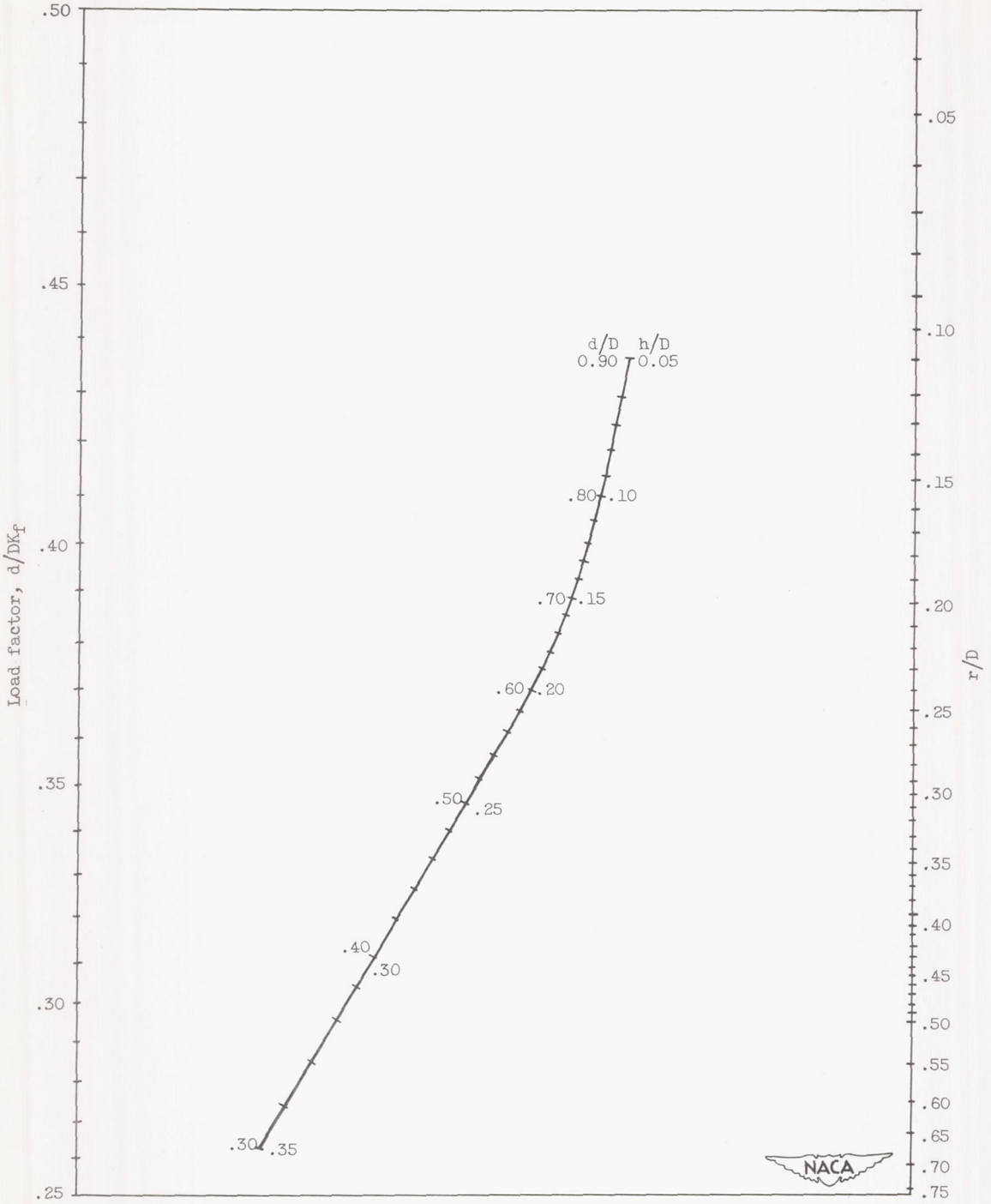

Figure 5. - Alinement chart for blade roots. D, over-all width; d, neck width; h, notch depth; r, notch radius.

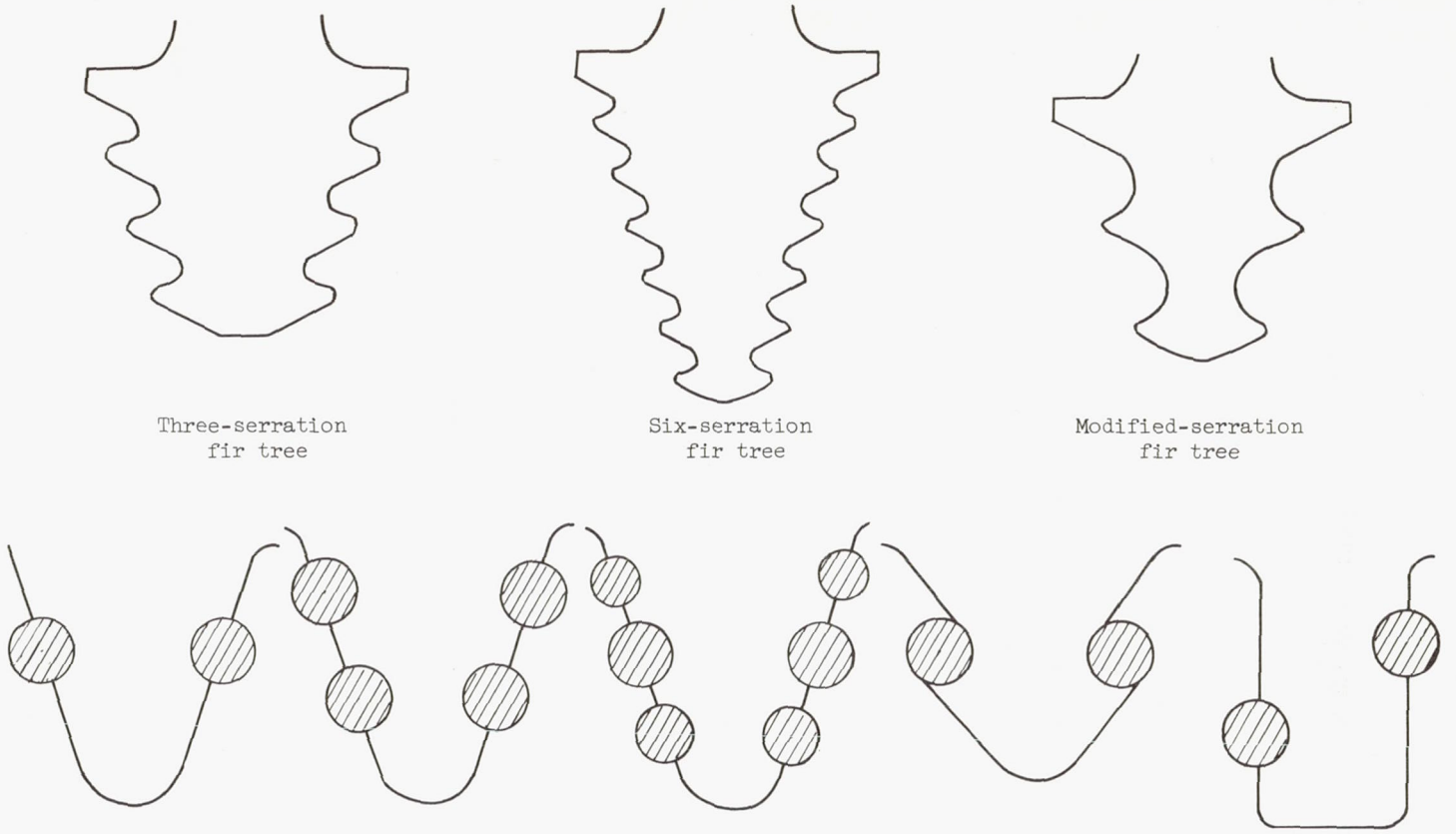

(a) Fir-tree and pin roots.

Figure 6. - Root profiles.

RESTRICTED

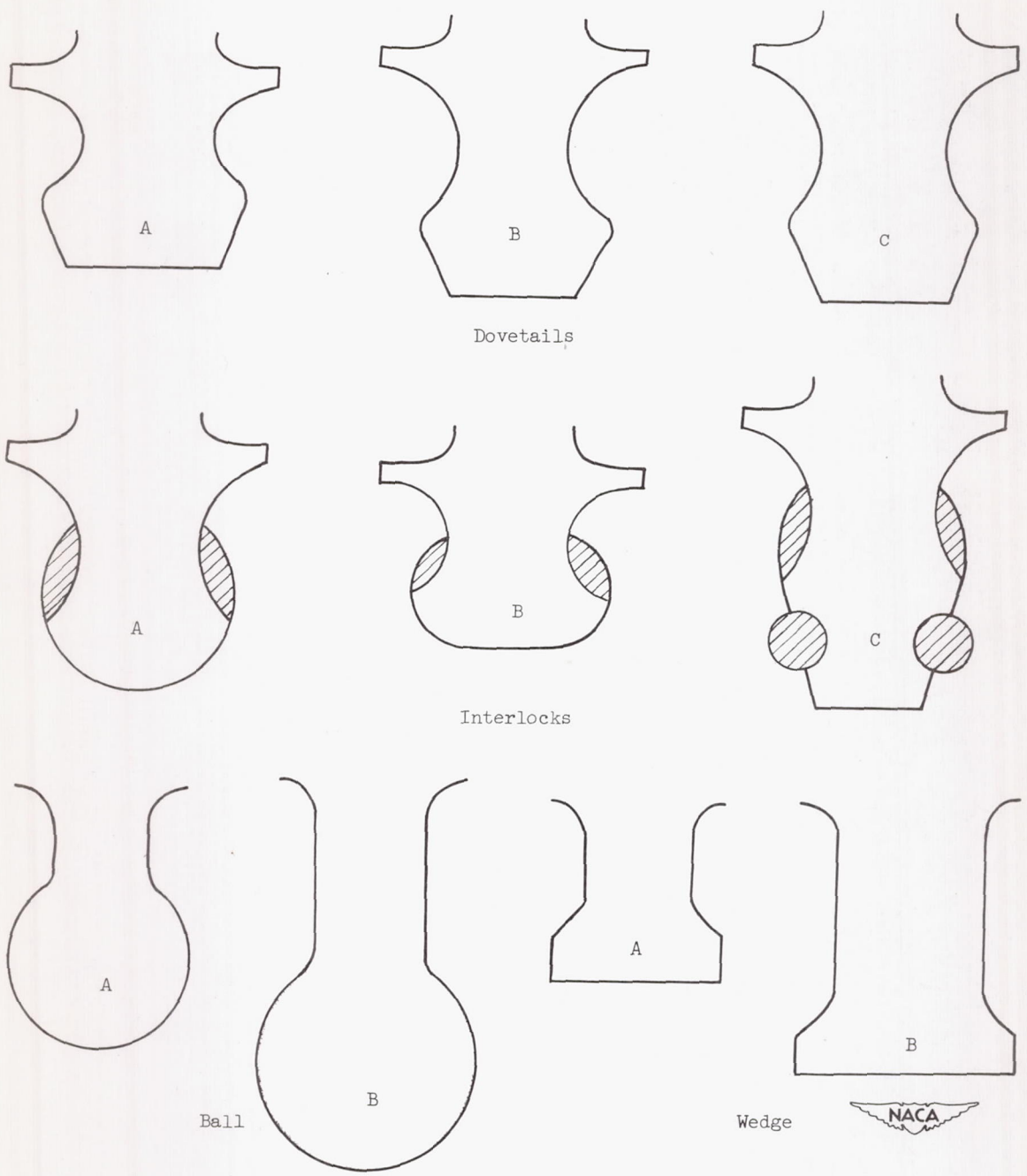

(b) Dovetail, interlock, ball, and wedge roots.

Figure 6. - Concluded. Root profiles.

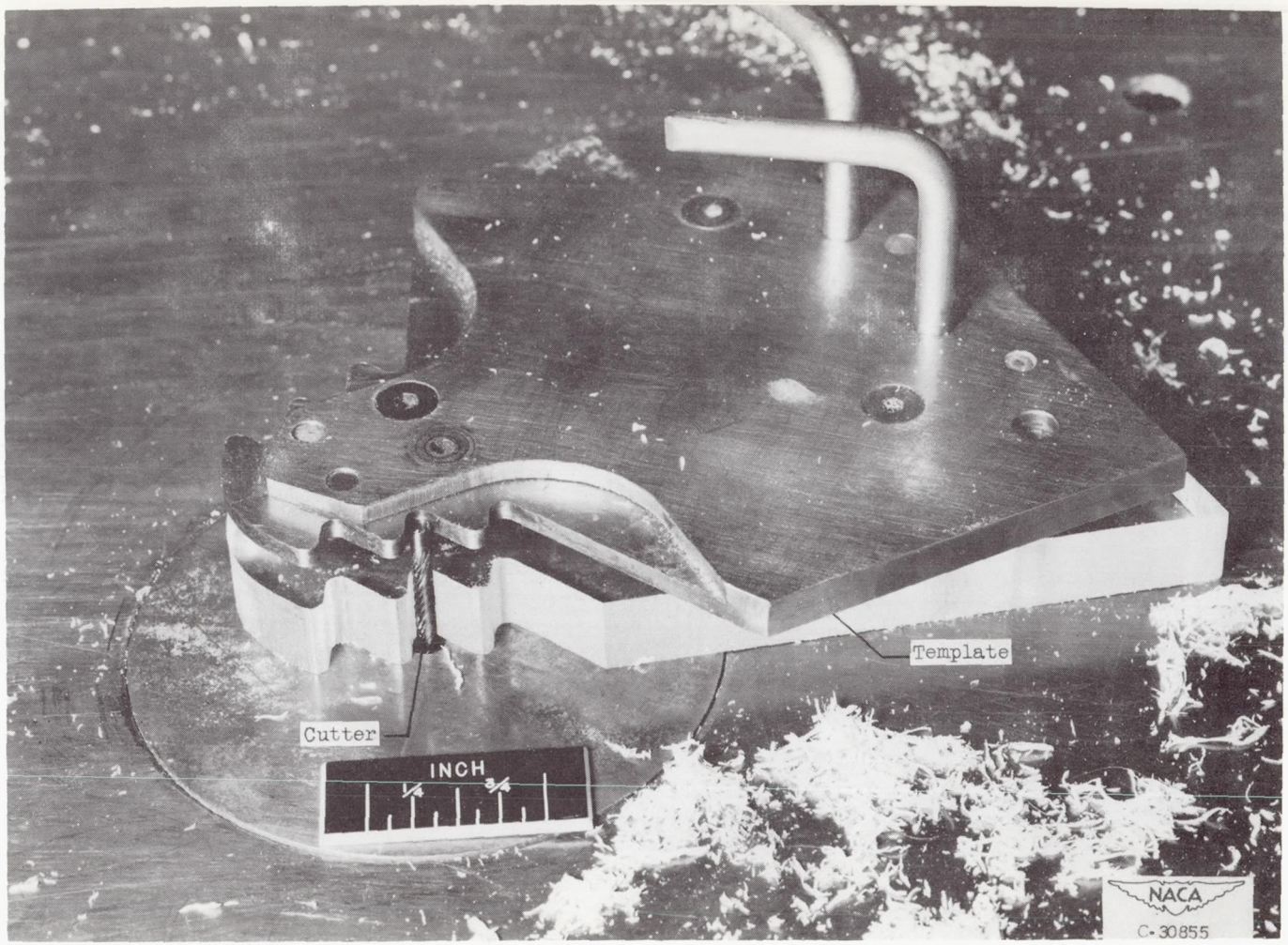

(a) By use of template for small radii.

Figure 7. - Routing of plastic blade-root model.

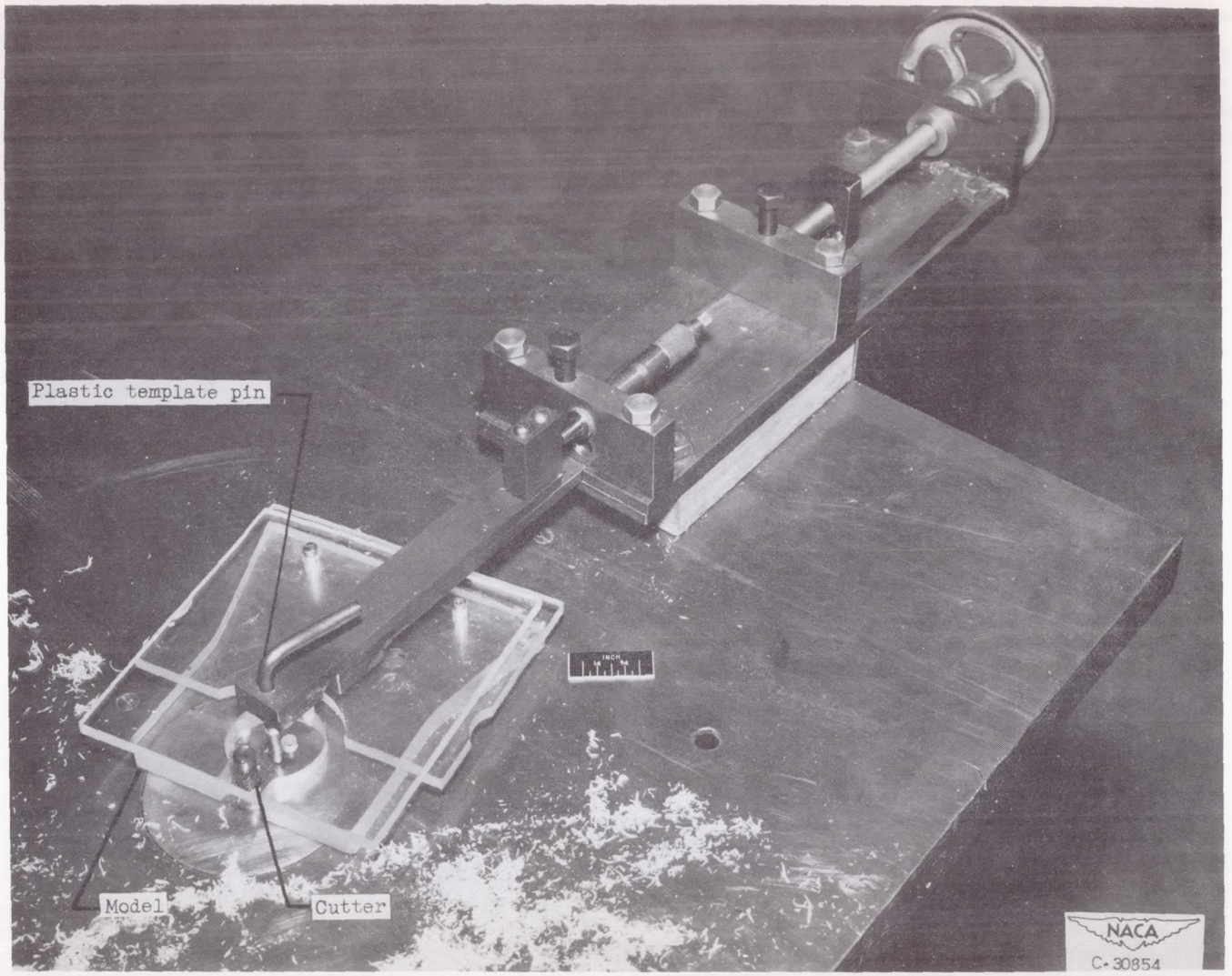

(b) By use of pivot template for large radii.

Figure 7. - Concluded. Routing of plastic blade-root model.

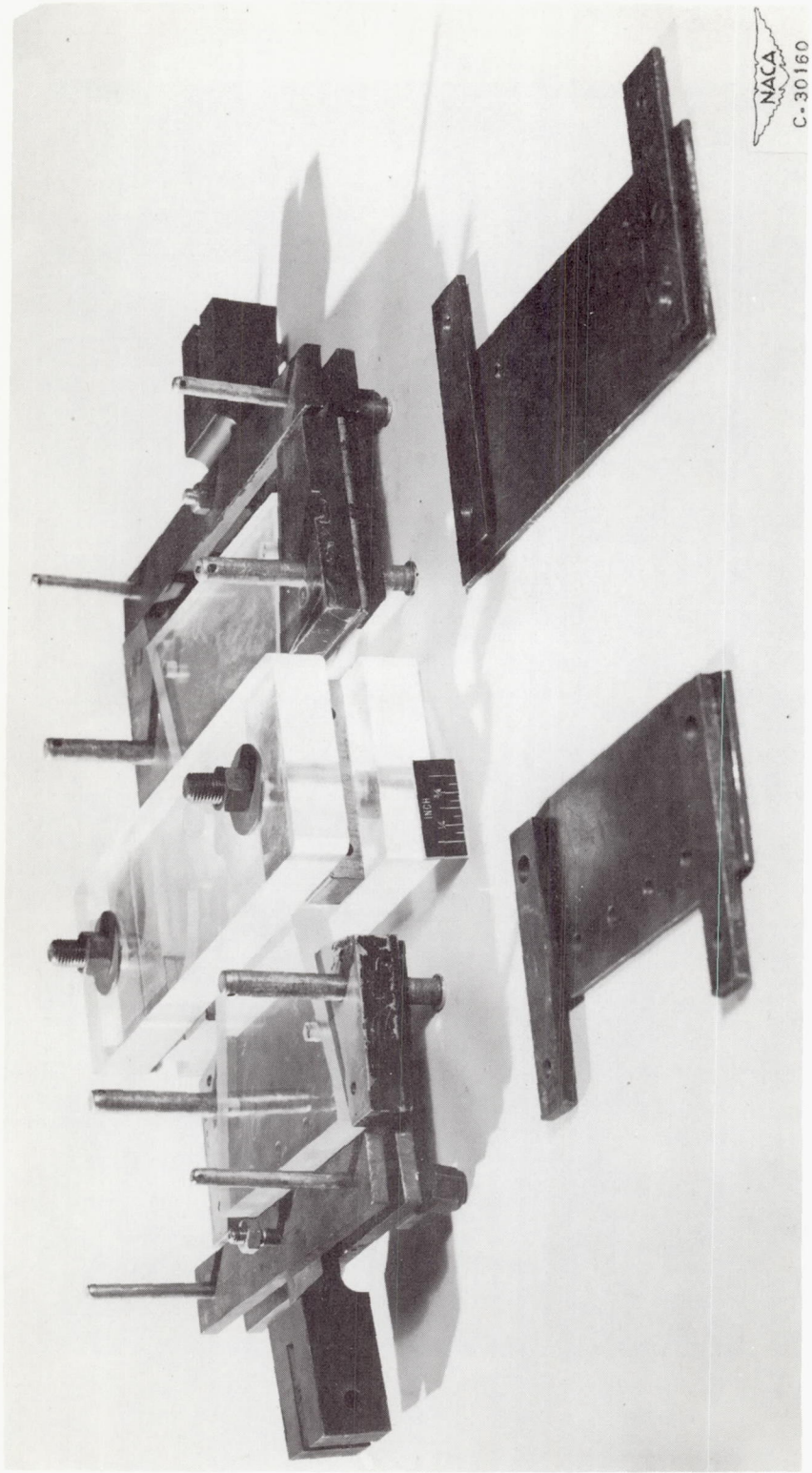

(a) Plastic blade-root model.

Figure 8. - Loading fixture.

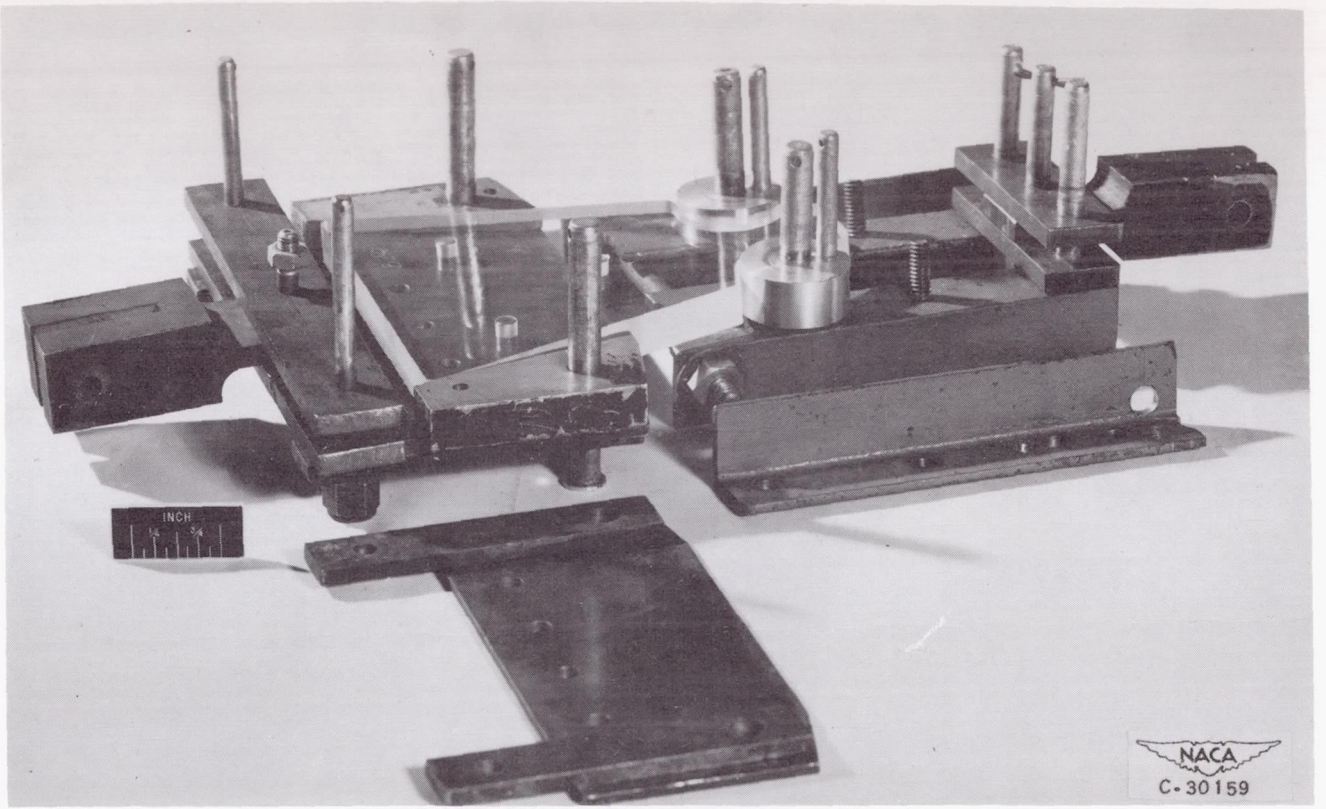

(b) Plastic notch-bearing specimens.

Figure 8. - Concluded. Loading fixture.

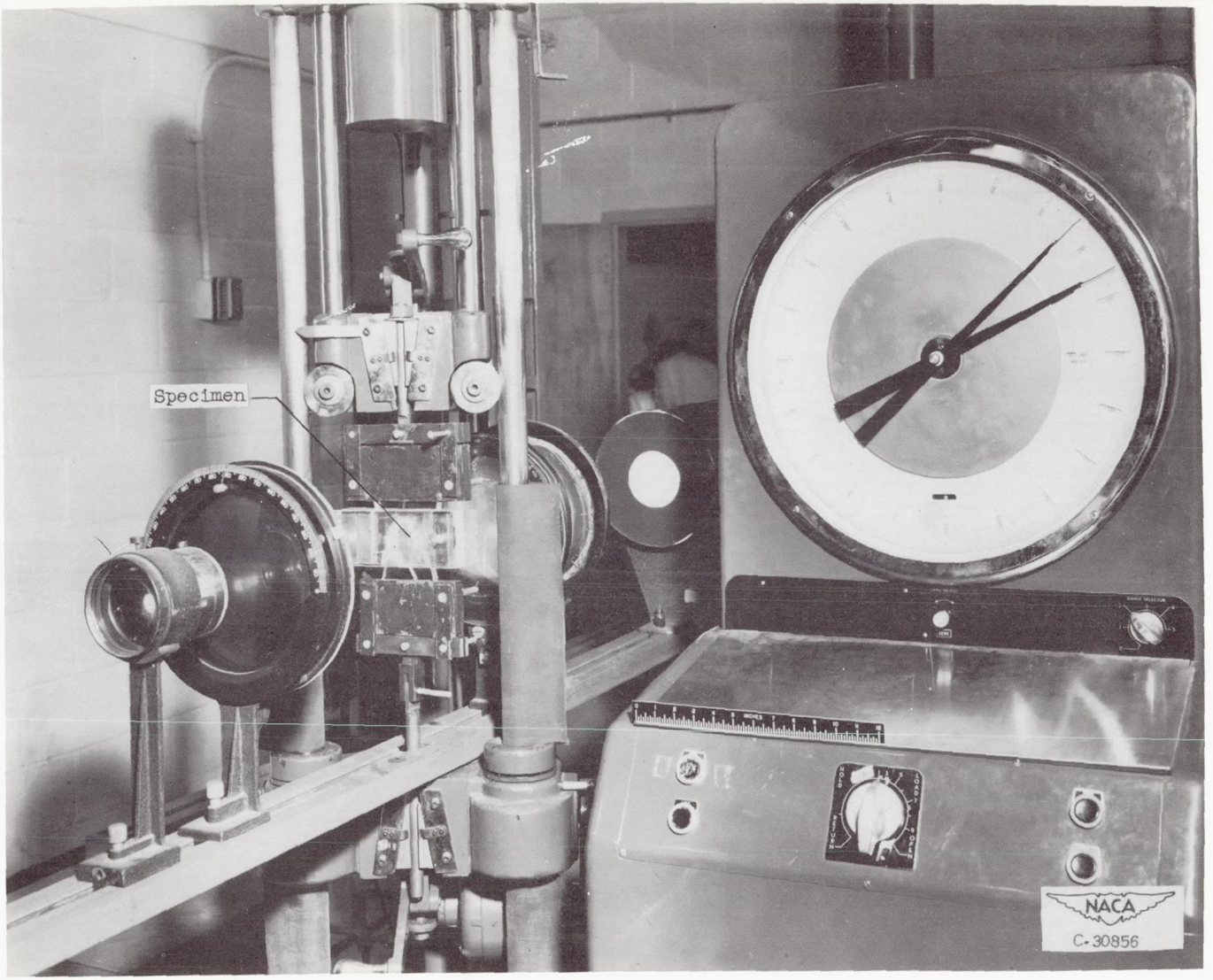

Figure 9. - Tensile machine and photoelastic apparatus used in testing models.

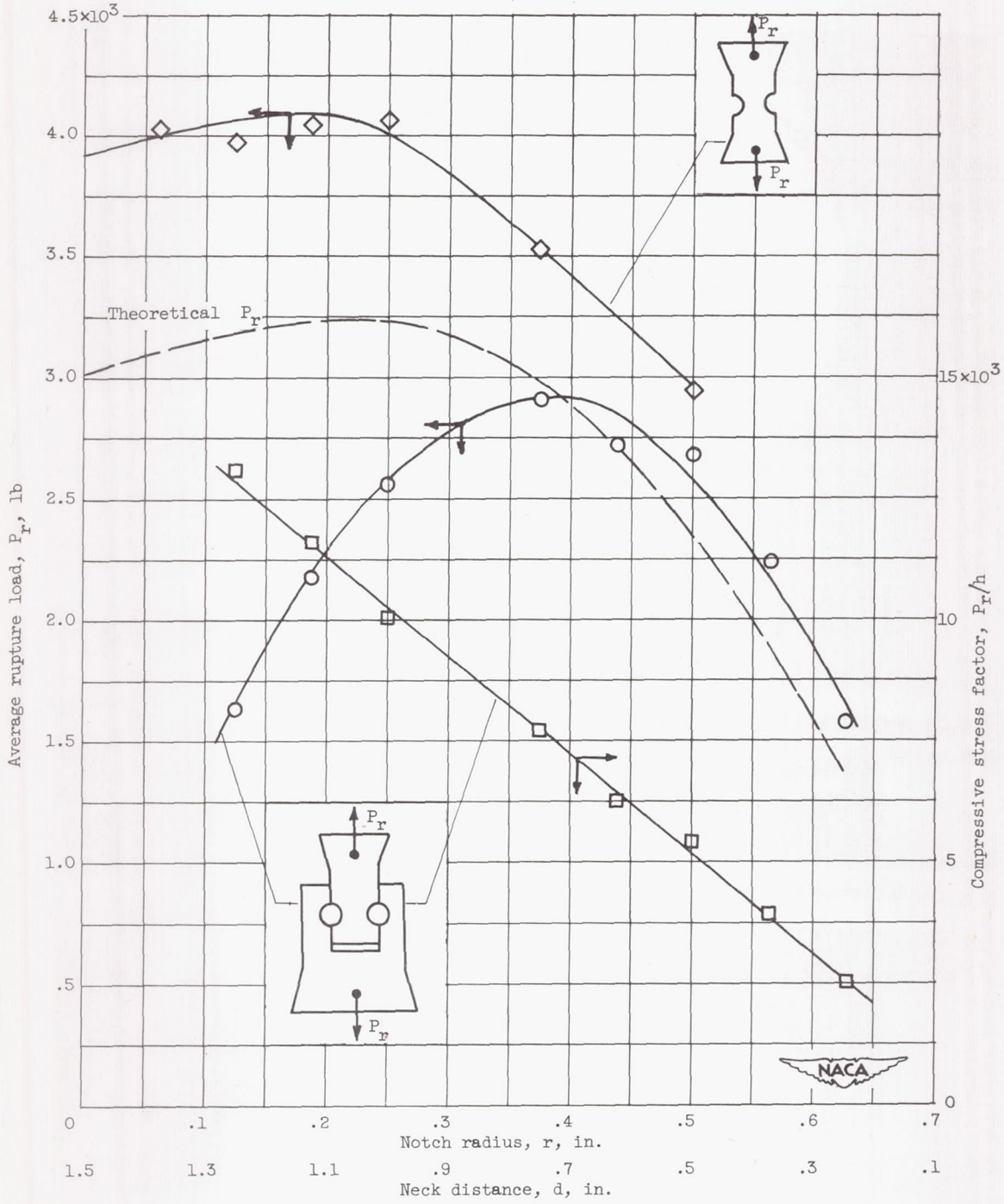

Figure 10. - Effect of method of loading on rupture load. Over-all width D, 1.5 inches.

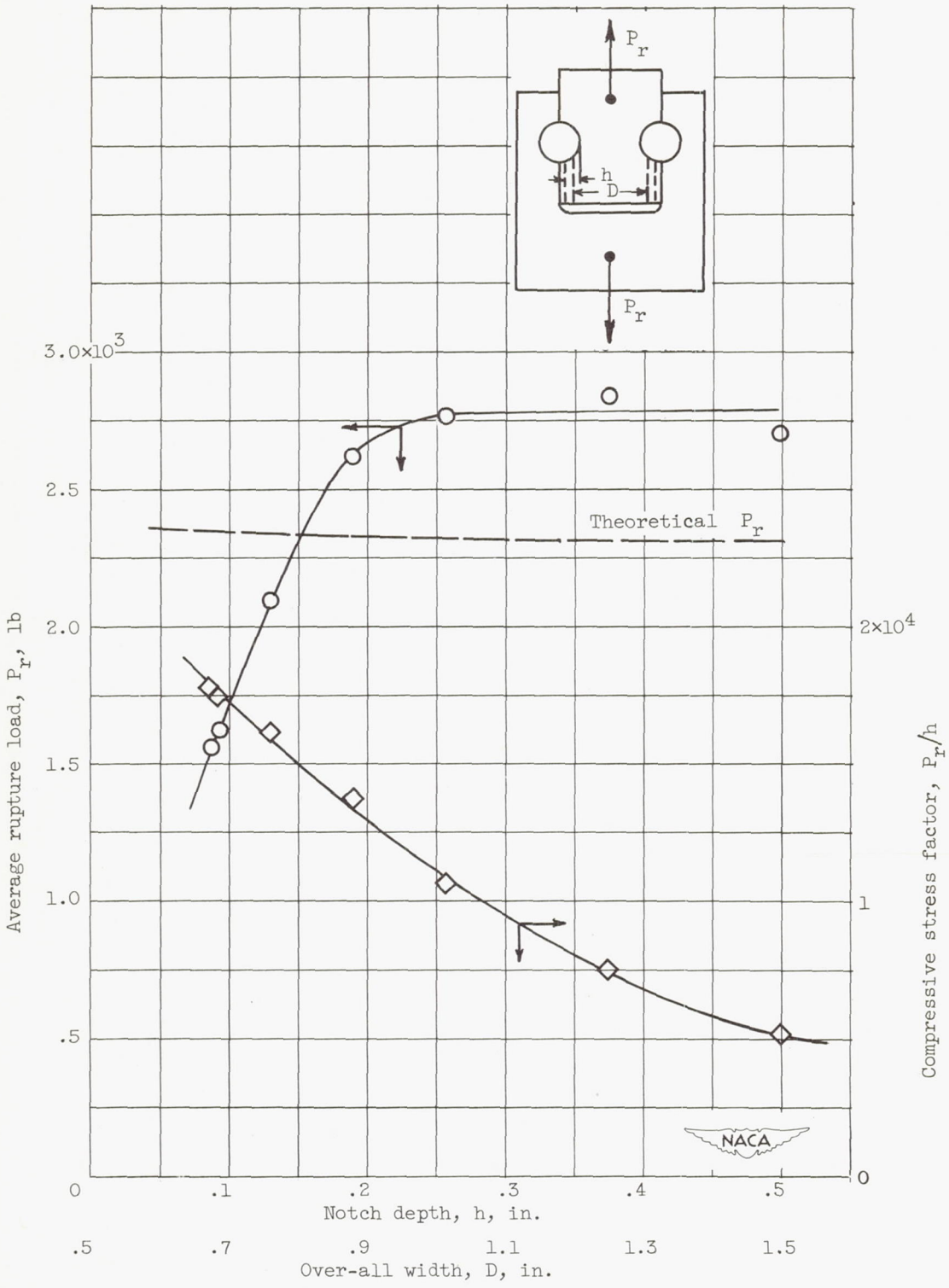

Figure 11. - Effect of varying only notch depth. Notch radius r, 0.5 inch; neck distance d, 0.5 inch.

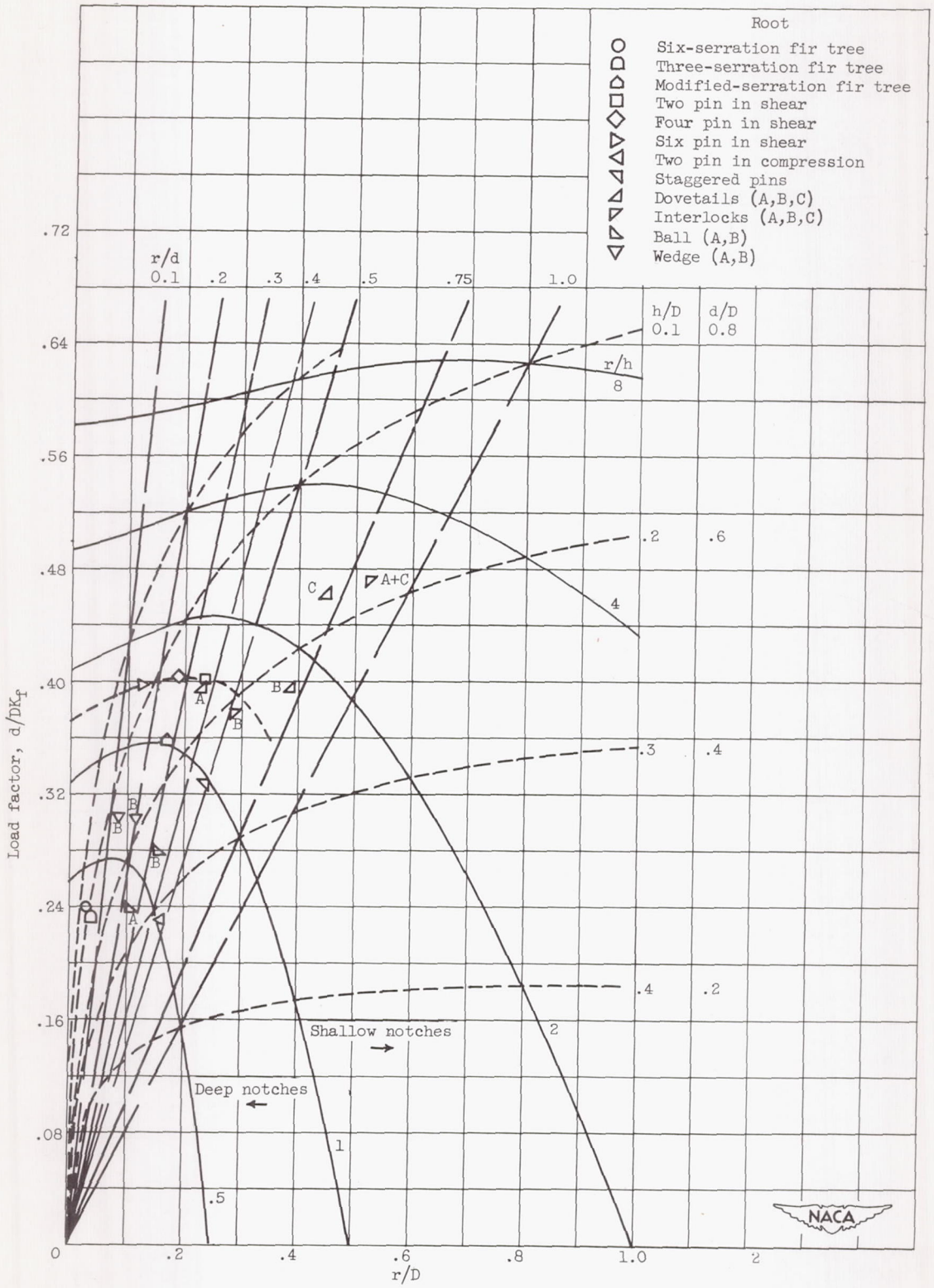

Figure 12. - Root designs plotted on combined theoretical chart. D, over-all width; d, neck width; h, notch depth; r, notch radius.

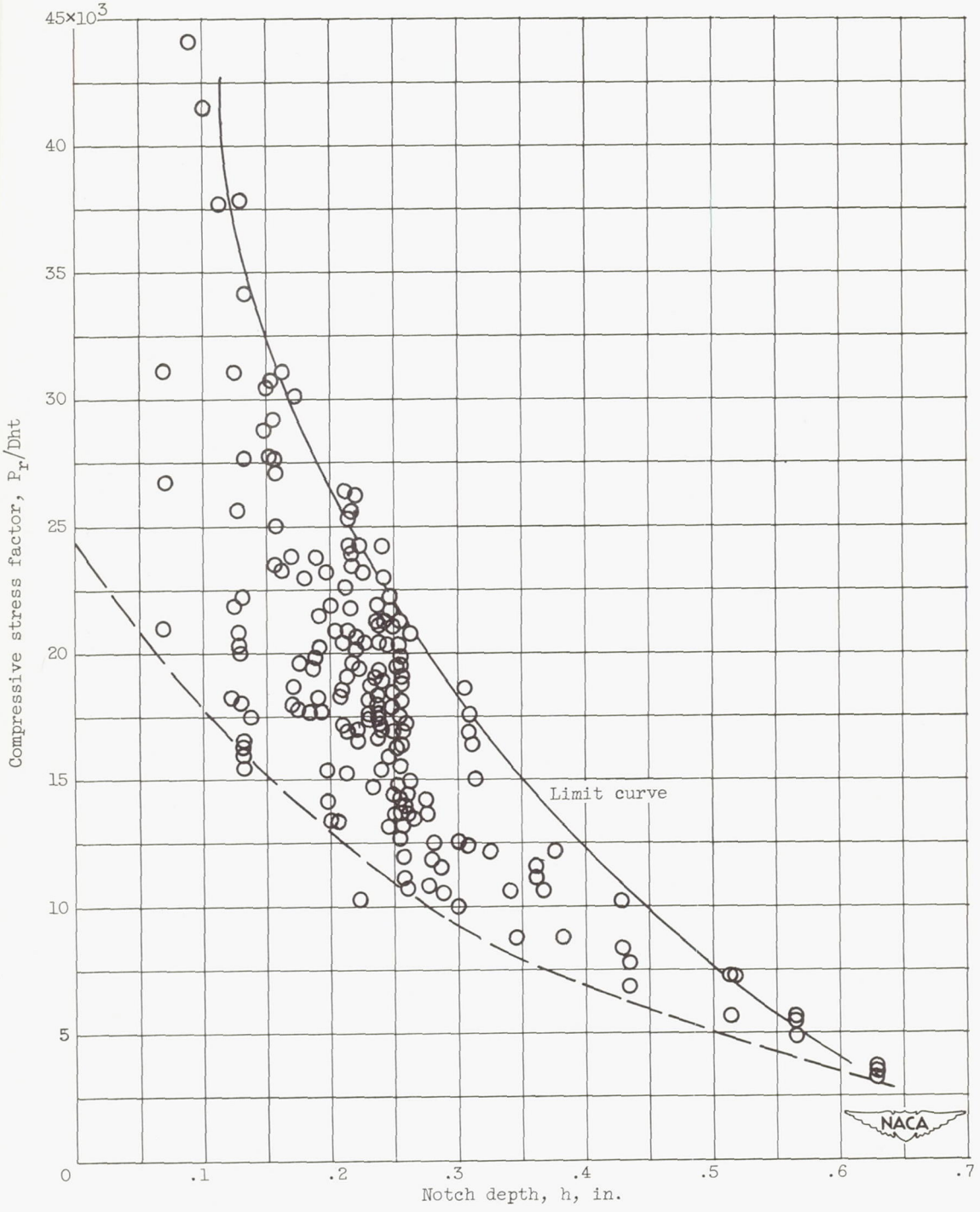

Figure 13. - Compressive stress of plastic specimens. D is variable.

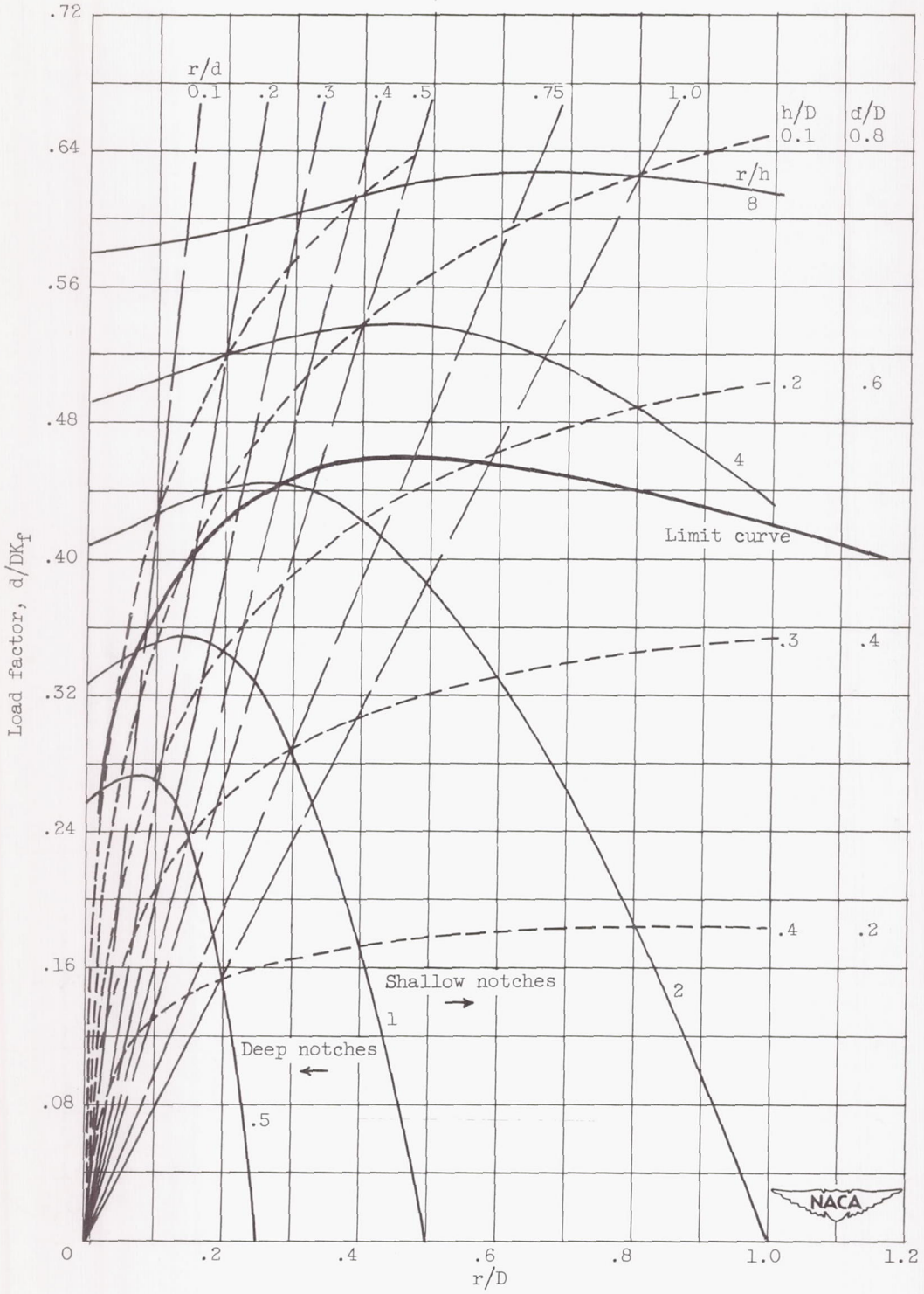

(a) Load factor against notch-radius parameter.

Figure 14. - Compressive-stress-limit curve on design chart. D, over-all width; d, neck width; h, notch depth; r, notch radius.

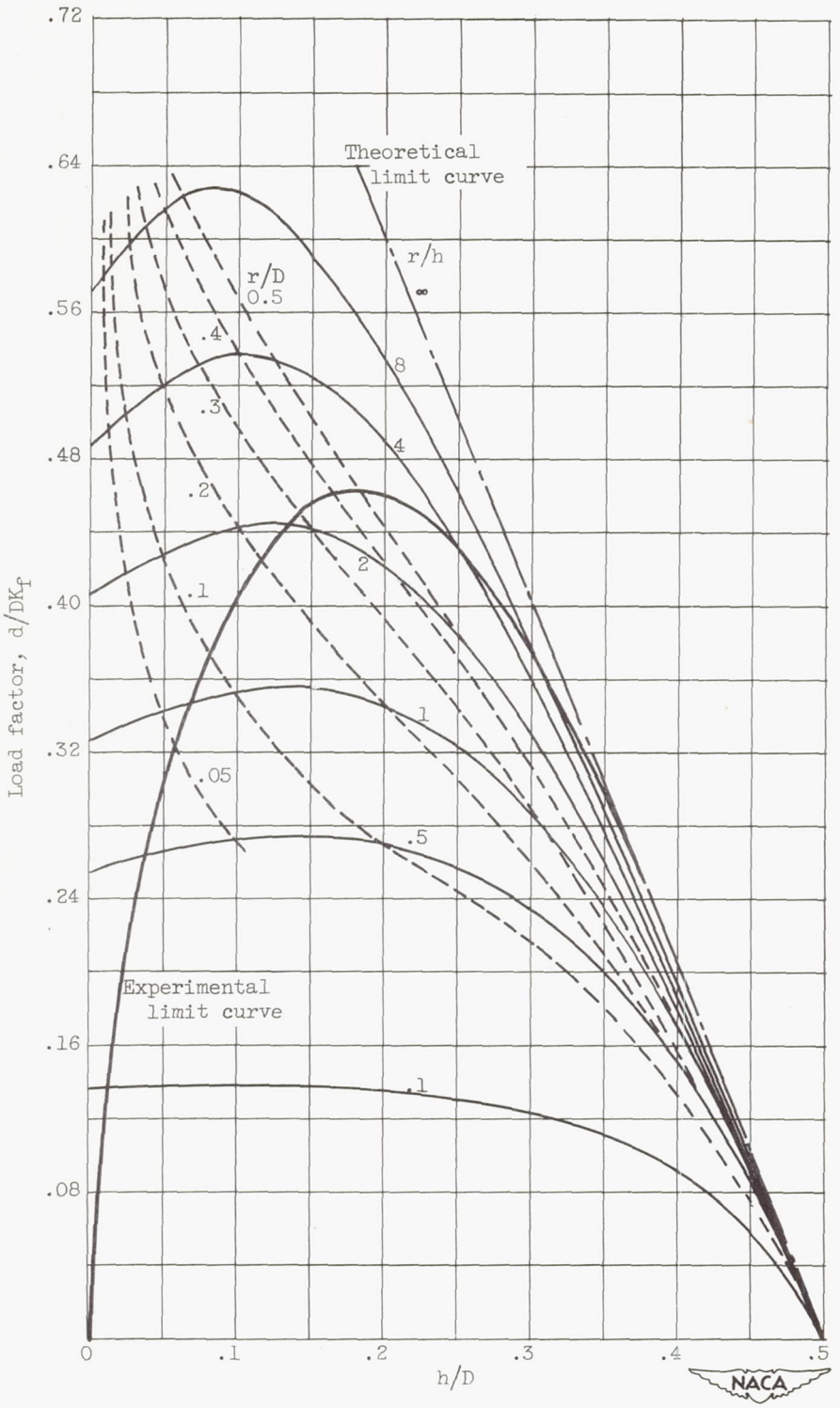

(b) Load factor against notch-depth parameter.

Figure 14. - Concluded. Compressive-stress-limit curve on design chart. D, over-all width; d, neck width; h, notch depth; r, notch radius.

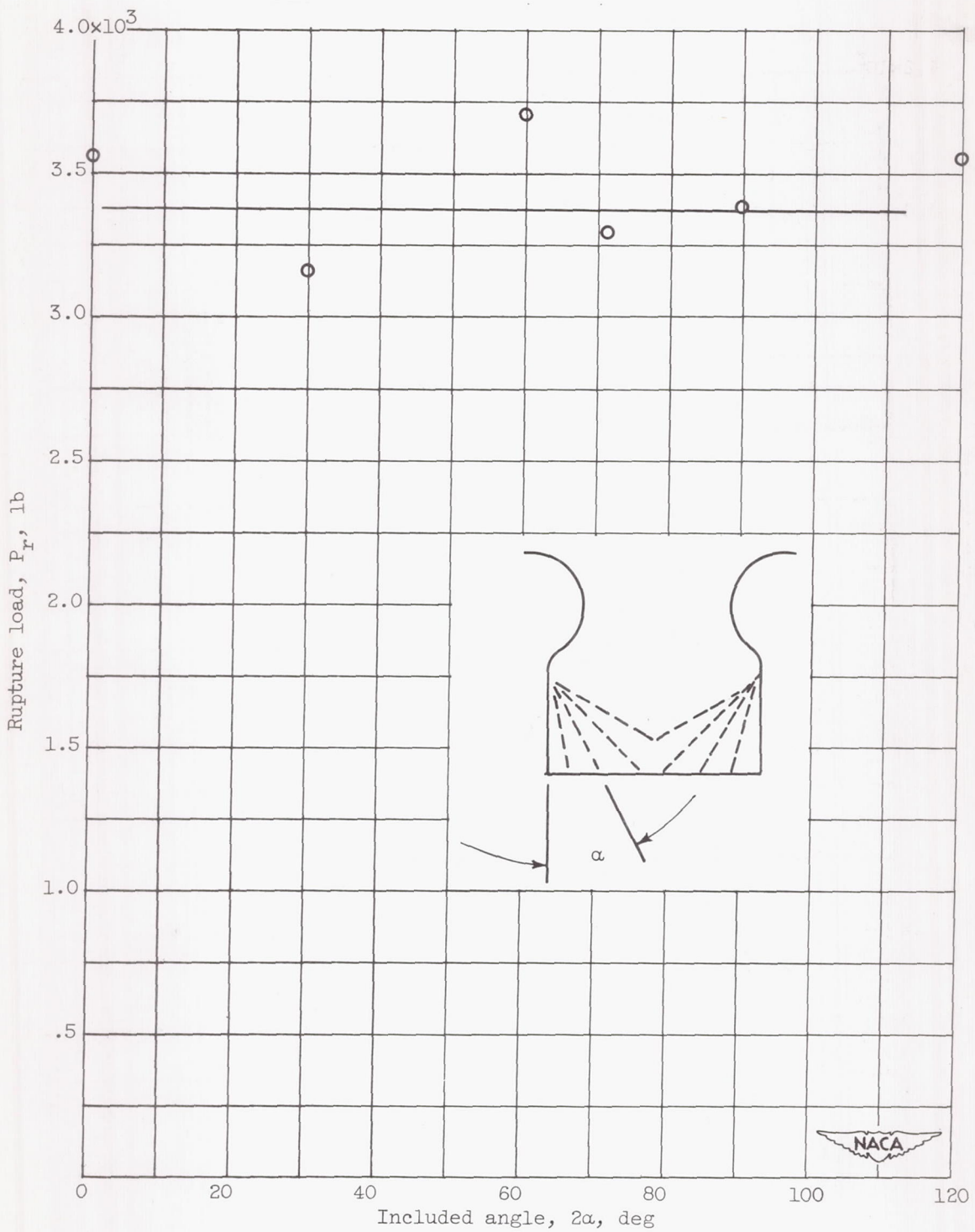

Figure 15. - Effect of varying included angle on dovetail-root strength.

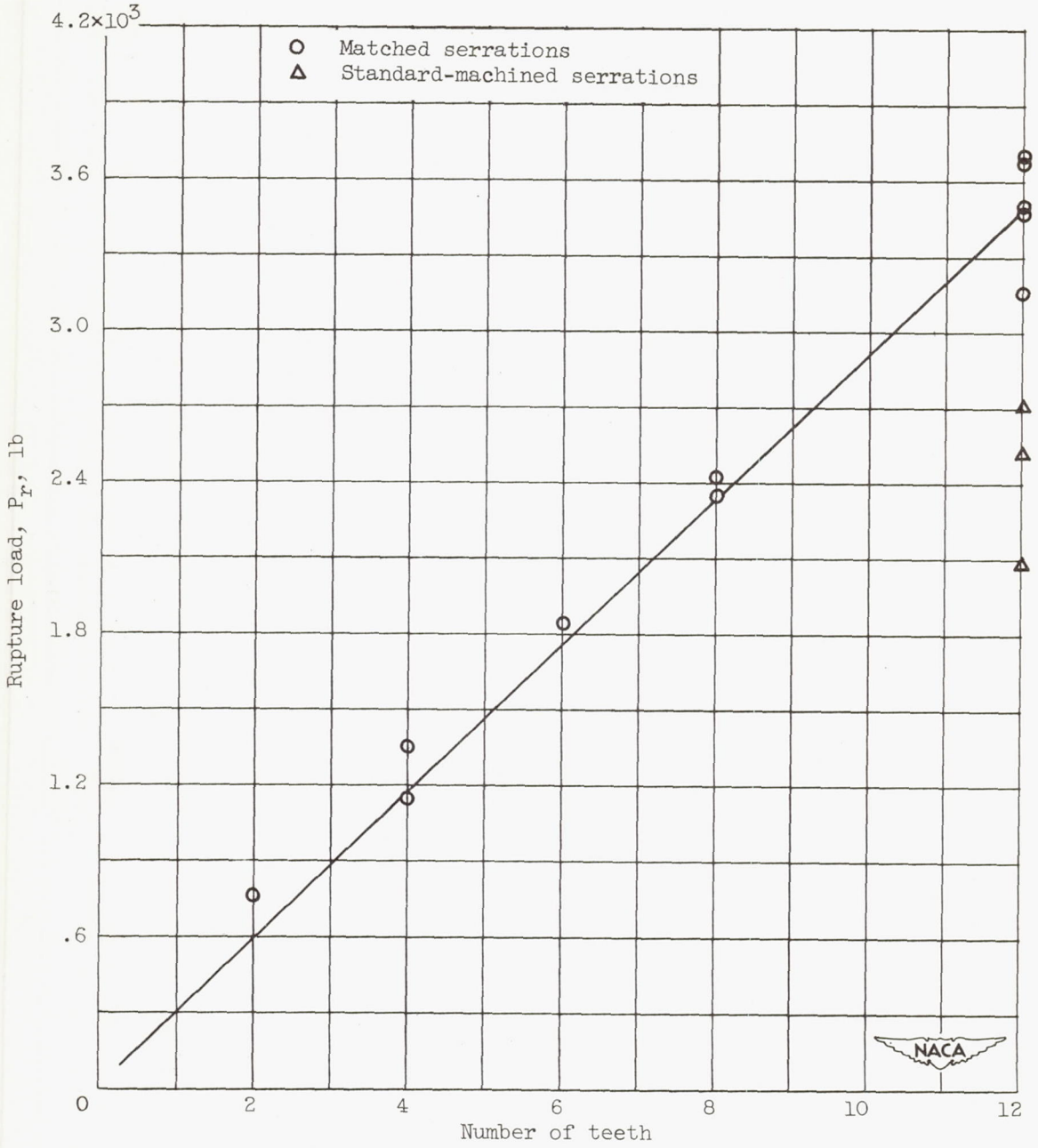

Figure 16. - Effect of additional lands. Neck distance d, 1.5 inches; thickness t, 0.5 inch.

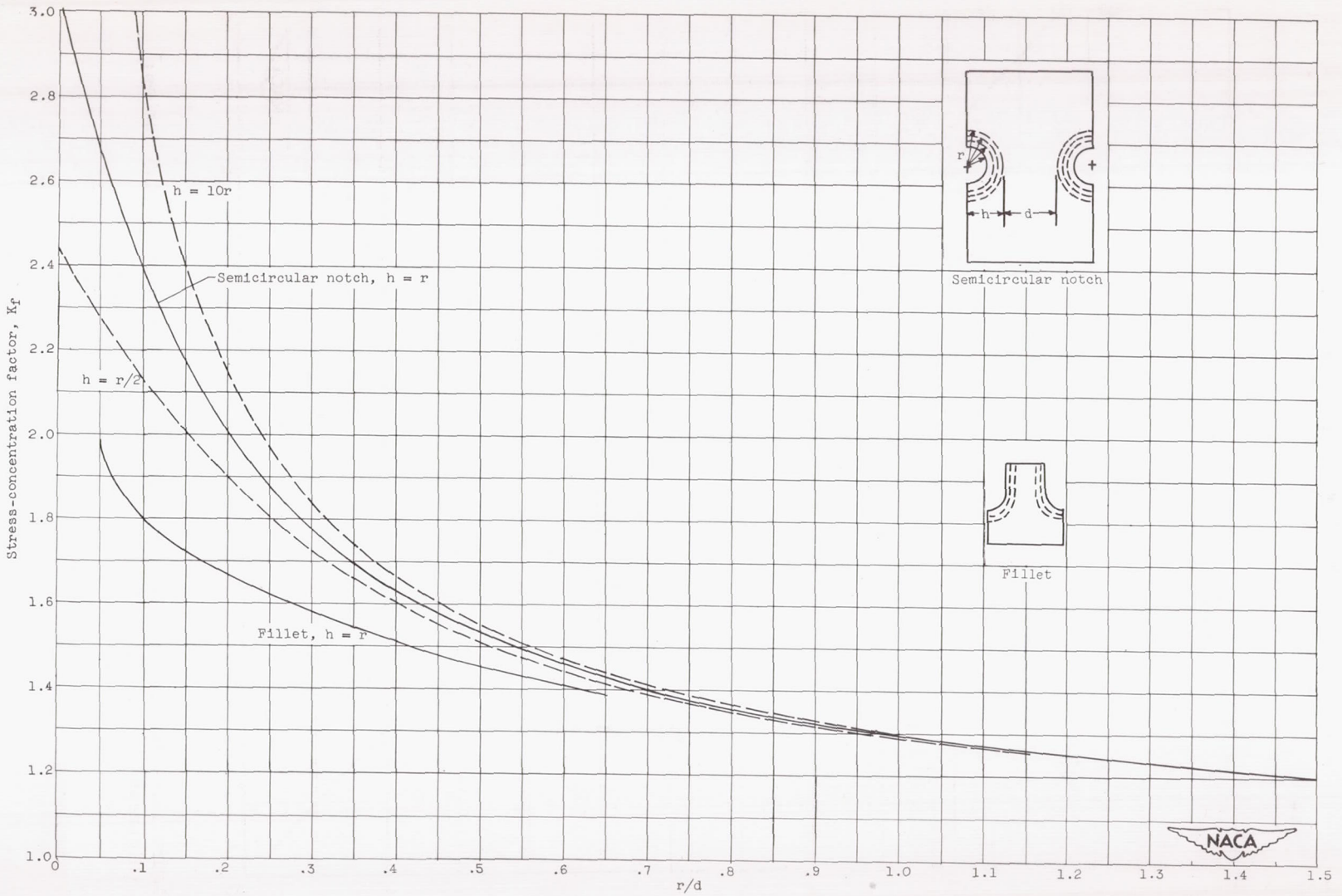

Figure 17. - Notch curves for h equal to r/2, r, and 10r.

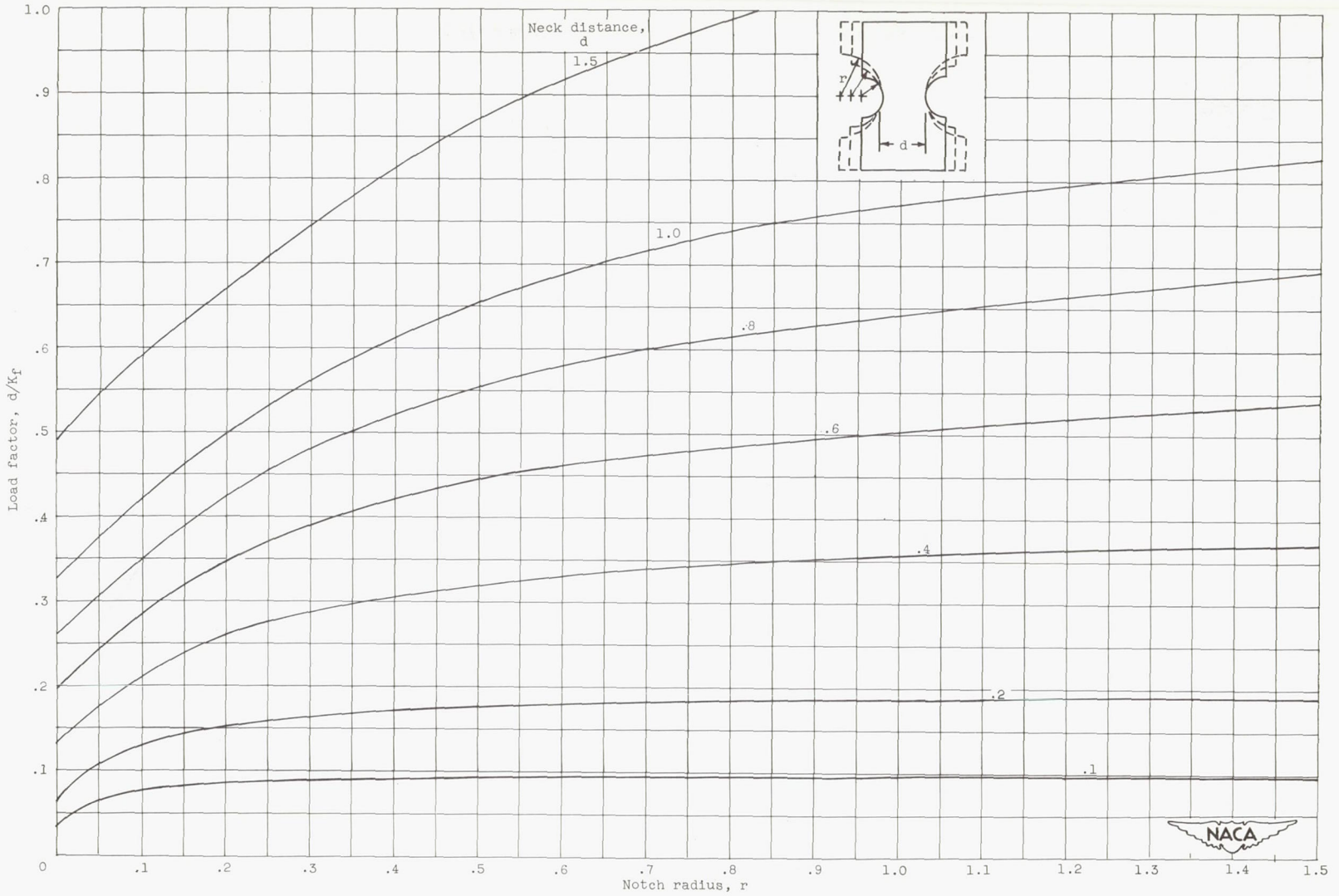

(a) Constant neck distance.

Figure 18. - Effects of varying root proportions on load factor. $P_r = \frac{d}{K_f} tS_t$. P_r, rupture load; t, thickness; S_t, tensile strength.

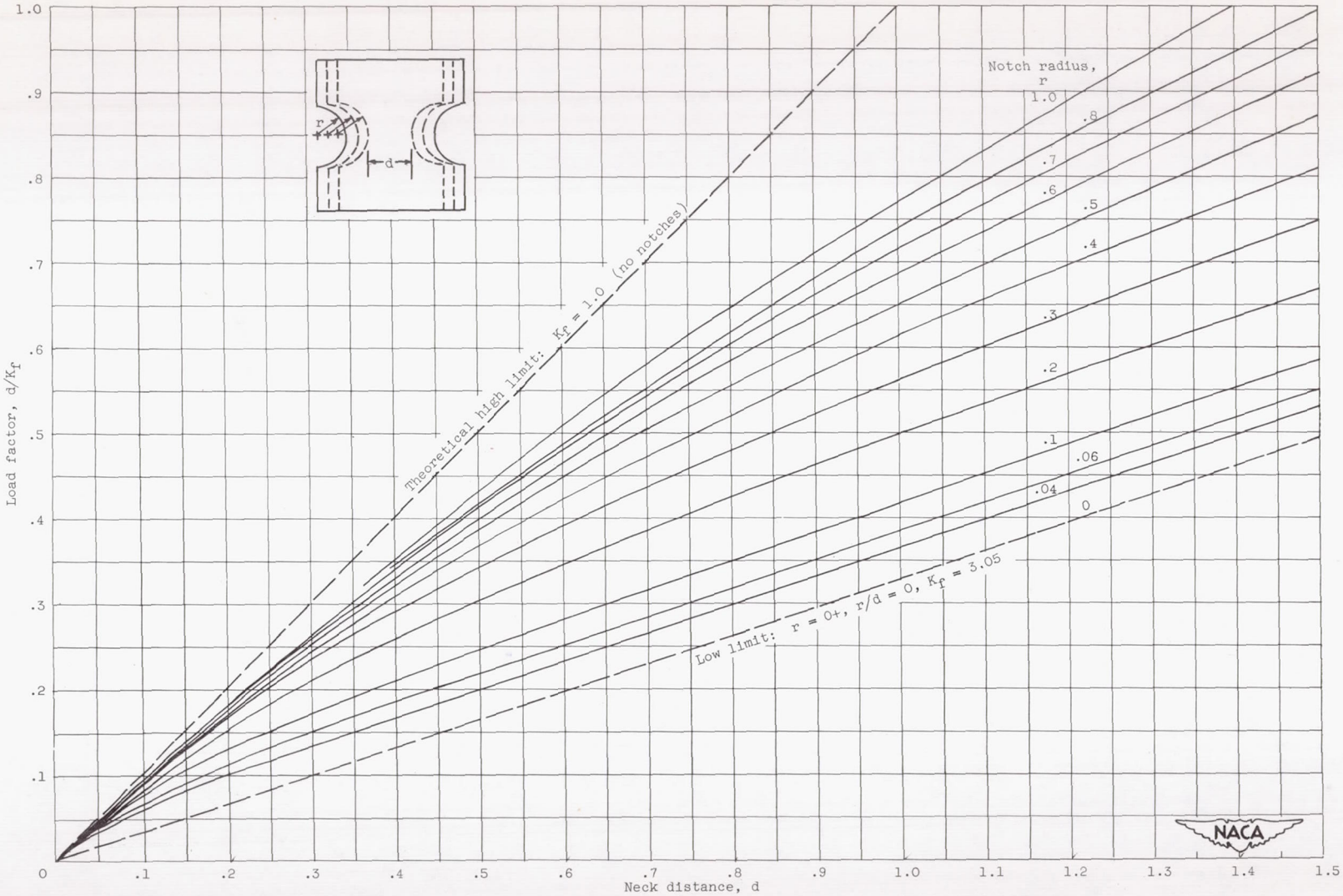

(b) Constant notch radius.

Figure 18. - Concluded. Effects of varying root proportions on load factor. $P_r = \frac{d}{K_f} tS_t$. P_r, rupture load; t, thickness; S_t, tensile strength.